Reprograming of sRNA target specificity by the leader peptide peTrpL in response to antibiotic exposure

Hendrik Melior[1], Siqi Li[1], Maximilian Stötzel[1], Sandra Maaß [ID][2], Rubina Schütz[1], Saina Azarderakhsh[1], Aleksei Shevkoplias[3,4], Susanne Barth-Weber[1], Kathrin Baumgardt[1], John Ziebuhr[5], Konrad U. Förstner [ID][6], Zoe Chervontseva[4], Dörte Becher [ID][2] and Elena Evguenieva-Hackenberg [ID][1,*]

[1]Institute of Microbiology and Molecular Biology, University of Giessen, 35392 Giessen, Germany, [2]Institute of Microbiology, University of Greifswald, 17489 Greifswald, Germany, [3]Faculty of Biology and Biotechnology, Higher School of Economics, 117312 Moscow, Russia, [4]Institute for Information Transmission Problems (the Kharkevich Institute, RAS), 127051 Moscow, Russia, [5]Institute of Medical Virology, University of Giessen, 35392 Giessen, Germany and [6]Data Science and Services, ZB MED - Information Centre for Life Sciences, 50931 Cologne, Germany

ABSTRACT

***Trans*-acting regulatory RNAs have the capacity to base pair with more mRNAs than generally detected under defined conditions, raising the possibility that sRNA target specificities vary depending on the specific metabolic or environmental conditions. In *Sinorhizobium meliloti*, the sRNA rnTrpL is derived from a tryptophan (Trp) transcription attenuator located upstream of the Trp biosynthesis gene *trpE(G)*. The sRNA rnTrpL contains a small ORF, *trpL*, encoding the 14-aa leader peptide peTrpL. If Trp is available, efficient *trpL* translation causes transcription termination and liberation of rnTrpL, which subsequently acts to downregulate the *trpDC* operon, while peTrpL is known to have a Trp-independent role in posttranscriptional regulation of antibiotic resistance mechanisms. Here, we show that tetracycline (Tc) causes rnTrpL accumulation independently of Trp availability. In the presence of Tc, rnTrpL and peTrpL act collectively to destabilize *rplUrpmA* mRNA encoding ribosomal proteins L21 and L27. The three molecules, rnTrpL, peTrpL, and *rplUrpmA* mRNA, form an antibiotic-dependent ribonucleoprotein complex (ARNP). *In vitro* reconstitution of this ARNP in the presence of competing *trpD* and *rplU* transcripts revealed that peTrpL and Tc cause a shift of rnTrpL specificity towards *rplU*, suggesting that sRNA target prioritization may be readjusted in response to changing environmental conditions.**

GRAPHICAL ABSTRACT
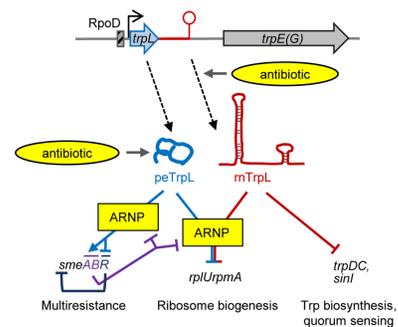
INTRODUCTION

In all studied organisms, small *trans*-acting RNAs (sRNAs) regulate gene expression by base pairing with mRNAs and influencing their translation and/or stability (1,2). Since many sRNAs bind to their mRNA targets by imperfect complementarity, they were often found to regulate multiple genes and rewire complex regulatory networks (3,4). However, even for sRNAs with multiple validated mRNA targets, usually much more target candidates were predicted, which, under given conditions, were found not to interact with the sRNAs (5,6). This raises the question whether some of those candidates are regulated by the sRNAs under alternative conditions.

In bacteria, features distinguishing mRNA targets from non-targets and targets prioritization were mostly studied in *Escherichia coli* on the example of sRNAs interacting with RNA chaperone Hfq (5,7). It was found that validated sRNA targets contain an Hfq binding site that does not overlap with the sRNA binding site. Furthermore, extent of

base-pairing and location of binding sites, as well as accessibility (no occlusion by secondary structures) of the sRNA and mRNA regions predicted to interact, were shown to be of major importance. Since changes in RNA structure are known to occur upon environmental changes (8) or upon binding of proteins or small molecules (9,10), it is conceivable that under changing conditions the sRNA specificity could be reprogramed.

The model organism *Sinorhizobium meliloti*, a soil alphaproteobacterium capable of fixing molecular nitrogen in symbiosis with legume plants, was shown to harbor many sRNAs (11). The subject of our study, the sRNA rnTrpL (previously RcsR1), is a highly conserved sRNA derived from the ribosome-dependent transcription attenuator of the tryptophan (Trp) biosynthesis gene *trpE(G)* (Figure 1A) (12–14).

The *trp* attenuator of Gram-negative bacteria relies on mutually exclusive secondary structures in the nascent RNA. The adopted structure depends on the translation efficiency of the small upstream ORF (uORF) *trpL*, which harbors consecutive Trp codons in its second half (15,16). If enough Trp is available, fast *trpL* translation allows the formation of stem loops (SL) 1 and 3, with SL3 acting as a transcription terminator (Figure 2A). In contrast, under conditions of insufficient Trp supply, transient ribosome pausing at the Trp codons prevents SL1 and SL3 formation. Instead, an antiterminator structure SL2 is formed, resulting in cotranscription of *trpL* with the downstream structural genes (15,17).

In contrast to *E. coli*, which has a single *trpEGDCFBA* operon, *S. meliloti* harbors three *trp* operons (Figure 1A–C), of which only the constitutively transcribed *trpE(G)* is regulated by attenuation (13,17). Recently, we have shown that under Trp replete conditions, when transcription is terminated downstream of *trpL*, the liberated sRNA rnTrpL binds in *trans* to the constitutively transcribed mRNA *trpDC*, leading to its destabilization (Figure 1B) (14). Additionally, rnTrpL destabilizes *sinI* mRNA encoding the autoinducer synthase gene (12), thus probably coordinating the quorum sensing onset with the cellular metabolism (Figure 1D). Also, the rnTrpL sRNA was predicted to interact with a range of other mRNAs (12), including *rplUrpmA* which encodes ribosomal proteins L21 and L27 (Figure 1E).

In addition to the rnTrpL sRNA, the *trp* attenuator of *S. meliloti* has a second *trans*-acting product, the leader peptide peTrpL (MANTQNISIWWWAR) that is encoded by *trpL* (Figure 1F). It has a Trp-independent role in resistance to tetracycline (Tc) and other substrates of SmeAB, the major multidrug resistance (MDR) efflux pump of *S. meliloti* (18). If bacteria growing in rich medium are exposed to Tc, peTrpL (i) strongly accumulates, (ii) binds in an antibiotic-dependent manner to an antibiotic-induced antisense RNA (asRNA) and (iii) causes a destabilization of the complementary *smeR* mRNA encoding the transcription repressor of *smeABR*, while *smeAB* mRNA is stabilized. This posttranscriptional mechanism involves the formation of antibiotic-dependent ribonucleoprotein complexes (ARNPs) containing peTrpL, the asRNA, *smeR* mRNA and Tc. It was shown that the *smeR*-ARNPs can be formed not only in the presence of Tc, but also of several other,

structurally different antimicrobial compounds that are extruded by SmeAB (18).

The role of peTrpL in multiresistance prompted us to consider a response of the *trp* attenuator to antibiotic exposure at the level of RNA. Indeed, the *trp* attenuator of Gram-negative bacteria is well suited to respond to translation inhibition by the release of rnTrpL, because in the absence of translation, the transcription terminator SL3 is formed (14,19,20). It is known that, under conditions of Trp availability, transcription termination at the attenuator is much stronger when *trpL* cannot be translated (21–24). This phenomenon is known as superattenuation (23). Thus, we decided to test whether the rnTrpL sRNA is generated upon exposure to translation inhibiting antibiotics such as Tc. We also tested whether rnTrpL plays a role in gene regulation in the presence of Tc and other translation inhibitors.

In this work, we show that the *S. meliloti trp* attenuator responds to Tc exposure by rnTrpL liberation. Furthermore, under conditions of Tc exposure, rnTrpL base pairs to and destabilizes the *rplUrpmA* mRNA. We provide evidence that for interaction with this mRNA, the rnTrpL sRNA operates in conjunction with the peTrpL peptide and translation inhibiting antibiotics that appear to reprogram the specificity of the sRNA. It is tempting to suggest that this mechanism saves resources required for the adaptation to antibiotic exposure in the soil habitat of *S. meliloti*.

MATERIALS AND METHODS

Cultivation of bacteria and exposure to antibiotics

Alphaproteobacterial strains (Supplementary Table S1) were cultivated semiaerobically (30 ml medium in a 50 ml Erlenmeyer flask or equivalent at 140 rpm and 30°C to an OD_{600} of 0.6) as previously described (18). *S. meliloti* was cultivated in rich TY medium (5 g BactoTryptone, 3 g Bacto-yeast extract, and 0.3 g CaC_2 per litre) (25) or GMX minimal medium (10 g D-mannitol, 5 g sodium glutamate, 5 g K_2HPO_4, 0.2 g $MgSO_4·7H_2O$, and 0.04 g $CaCl_2$ per litre; trace elements: 0.05 mg $FeCl_3·6H_2O$, 0.01 mg H_3BO_3, 0.01 mg $ZnSO_4·7H_2O$, 0.01 mg $CoCl_2·6H_2O$, 0.01 mg $CuSO_4·5H_2O$, 1.35 mg $MnCl_2$, and 0.01 mg $Na_2MoO_4·2H_2O$ per litre; 10 μg biotin and 10 mg thiamine per litre) (26). TY medium was also used for *Agrobacterium tumefaciens*, while *Bradyrhizobium japonicum* was cultivated in PSY medium (300 mg KH_2PO_4, 300 mg Na_2HPO_4, 5 mg $CaCl_2$, 100 mg $MgSO_4$, 3 g peptone, 1 g yeast extract, 10 mg H_3BO_3, 1 mg $ZnSO_4$, 0.5 mg $CuSO_4$, 0.1 mg Na_2MoO_4, 0.1 mg $MnCl_2$, 0.19 mg $FeCl_3$, 1 mg thiamine–HCl, 1 mg biotin, 1 mg Na-panthothenate, and 1 g L-arabinose/l) (27). When strains harboring respective resistance plasmids were grown in liquid cultures, Tc and gentamycin (Gm) were used at final concentrations of 20 μg/ml and 10 μg/ml, respectively. Strains lacking such plasmids were exposed to subinhibitory Tc concentration (1.5 μg/ml). The same volume of the solvent ethanol (60 μl) was added to the 50 ml control cultures. Other antibiotics were used at the following subinhibitory concentrations: 27 μg/ml erythromycin (Em), 9 μg/ml chloramphenicol (Cl), 3 μg/ml rifampicin (Rf) and 45 μg/ml kanamycin (Km).
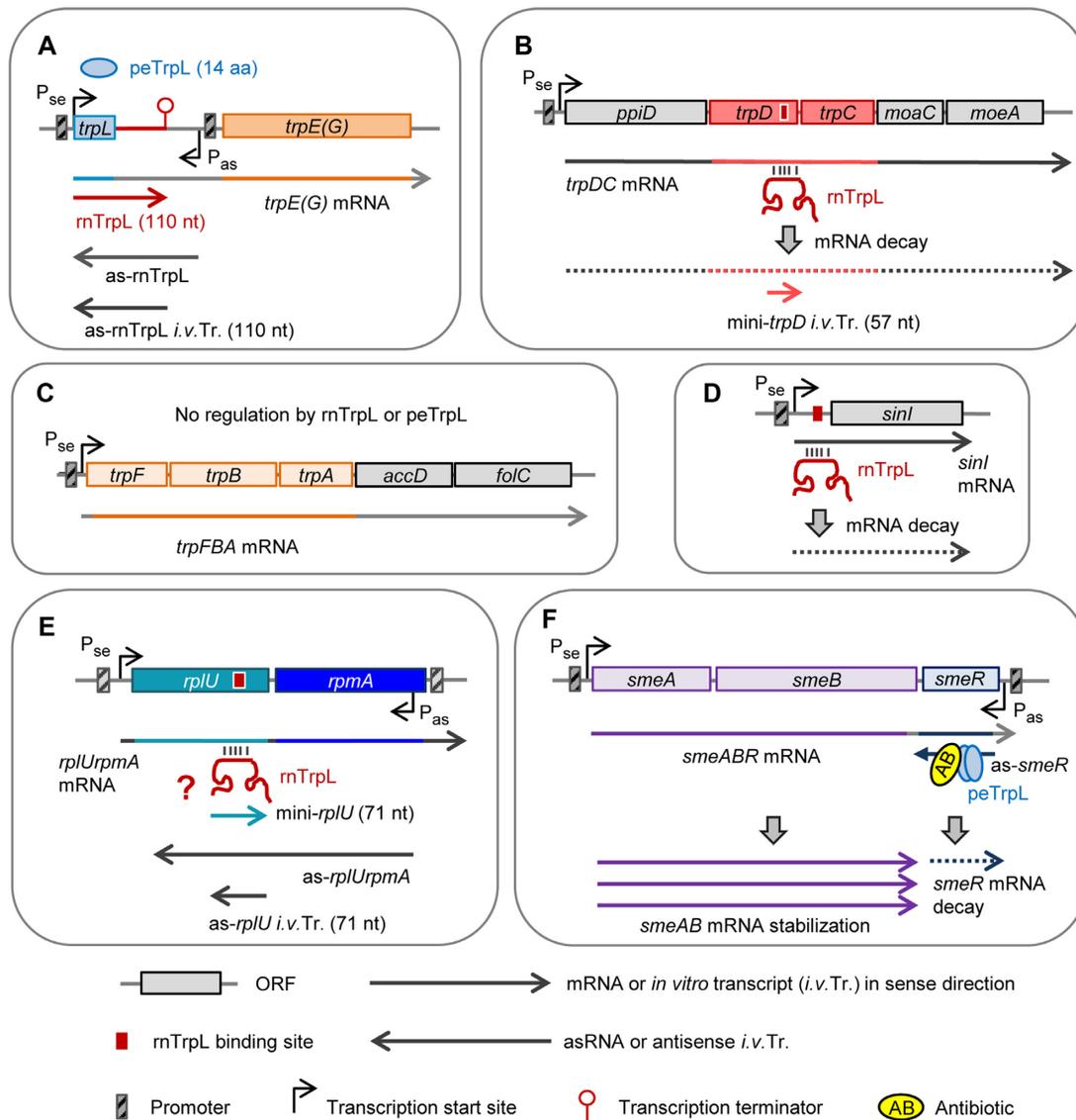
Figure 1. The three *trp*-operons in *S. meliloti* 2011 and operons targeted by rnTrpL and/or peTrpL in *trans*. P_{se}: sense promoter, P_{as}: antisense promoter. (**A**) The *trpE(G)* operon and its products rnTrpL and peTrpL (13). (**B**) The *trpDC* operon and its regulation by rnTrpL. The rnTrpL sRNA base pairs with a specific mRNA region and destabilizes the polycistronic transcript (14). (**C**) The *trpFBA* operon, which is not regulated by rnTrpL or peTrpL (14). (**D**) The *sinI* gene and its posttranscriptional regulation by rnTrpL (12). (**E**) The *rplUrpmA* operon and the proposed binding of rnTrpL to a specific region in the *rplU* coding region. (**F**) The *smeABR* operon and its differential, posttranscriptional regulation by peTrpL. The peTrpL peptide forms an ARNP complex with the as-*smeR* RNA and the *smeR* segment of the *smeABR* mRNA. This leads to destabilization of the *smeR* mRNA segment, while the *smeAB* segment is stabilized (18). Transcription start sites (TSSs) and corresponding promoters are indicated either according to (13,14,18,38) or to results of this study. In a previous, transcriptome-wide TSS analysis (41), the antisense TSS downstream of rnTrpL was mapped, while the antisense TSS at the end of *rpmA* was not. The indicated TSS of as-*rplUrpmA* corresponds to a major 5′-end identified by RNA-Seq of coimmunoprecipitated RNA (18). The 3′-ends of the asRNAs were not determined. Their estimated length was inferred from the RNA-Seq analysis of coimmunoprecipitated RNA (18).

Cloning procedures, conjugation, induction and fluorescence measurement

Cloning in *E. coli* and transfer of plasmids by conjugation into *S. meliloti* was conducted by standard methods (28) and as described previously (14). Plasmids and oligonucleotides are listed in Supplementary Table S1 and Supplementary Table S2, respectively. The pRK4352-derived plasmids confer Tc resistance and enable constitutive transcription (29). The plasmids pSRKGm and pSRKTc (conferring resistance to Gm and Tc, respectively) allow for IPTG-induced transcription in Alphaproteobacteria (30). Unless

indicated otherwise, induction with 1 mM IPTG was performed for 10 min. Fluorescence of strains producing L27′-EGFP fusion protein was measured using a Tecan Infinite M200 reader. Values were normalized to the ODs and to the fluorescence of empty vector control (EVC) cultures.

RNA purification

The RNA purification methods used in this work were previously described (14,18). Briefly, total RNA for northern blot hybridization and determination of RNA steady-

state levels by qRT-PCR was purified by TRIzol and subsequent hot-phenol treatment. For determination of mRNA half-lives by qRT-PCR, RNA was purified after rifampicin treatment using RNAprotect Bacteria Reagent and RNeasy columns (Qiagen).

Real time RT-PCR (qRT-PCR)

Prior to qRT-PCR analysis, 10 μg RNA was treated with 1 μl TURBO-DNase for 30 min and success of DNA removal was confirmed by PCR with *rpoB*-specific primers for each sample (40 ng RNA was used in a 10 μl reaction mixture; 40 ng total DNA was used in a positive control reaction). RNA was diluted to 20 ng/μl and 2 μl of a diluted sample were used for strand-specific qRT-PCR conducted with Brilliant III Ultra Fast SYBR® Green QRT-PCR Mastermix containing the polymerase enzymes (Agilent). First, 9 μl reaction mixtures containing 10 pmol of the reverse primer were assembled. After cDNA synthesis, the reverse transcriptase was inactivated, the forward primer was added, and real-time PCR was performed in a spectrofluorometric thermal cycle (Bio-Rad). The quantification cycle (Cq) was set to a value at which the curvature of the amplification was maximal using Bio-Rad CFX Manager 3.0. When the technical duplicates differed by >0.5 Cq, the qRT-PCR was repeated. No-template-controls were always included, and the specificity of the qPCR product was validated by a melting curve after the qPCR-reaction.

Routinely, each qRT-PCR sample contained 40 ng RNA and *rpoB* mRNA was used as reference. However, when 16S rRNA was used as a reference, the RNA samples were additionally diluted (0.004 ng RNA was used in a 10 μl reaction mixture) to obtain similar Cq of mRNA and 16S rRNA. Primer pair efficiency (Supplementary Table S2) was determined by PCR using serial two-fold dilutions of RNA.

For studying changes in cellular mRNA levels, the analysis of the gene of interest and of the reference gene were performed with portions of the same total RNA sample, and two samples were compared by calculating fold changes of RNA levels with the Pfaffl formula (31). For calculating the enrichment by coimmunoprecipitation (CoIP) or affinity chromatography, the qRT-PCR of the gene of interest was performed with coimmunoprecipitated- or copurified-RNA sample, while total RNA of the same culture (harvested prior to cell lysis) was used for the *rpoB* qRT-PCR. Then, the Pfaffl formula was used to calculate the fold enrichment in comparison to the corresponding mock control. All qRT-PCR graphs show means and standard deviations from three independent experiments, each performed in technical duplicates.

In vitro transcription

In vitro transcription was performed using the MEGAshortscript T7 kit as described (18). Either PCR products with integrated T7 promoters were used as templates, or complementary oligonucleotides were annealed to obtain a double-strand, T7 promoter containing template. The used oligonucleotides are listed in Supplementary Table S2. To synthesize non-labeled transcripts, 500 ng template, $1\times$ T7-polymerase buffer,

7.5 mM ATP, 7.5 mM CTP, 7.5 mM GTP, 7.5 mM UTP and 25 U T7-enzyme mix were used. Internally labeled transcripts were synthesized using 0.5 mM ATP, 0.5 mM CTP, 0.5 mM GTP, 0.1 mM UTP and 2 μl [α-^{32}P]-UTP (10 μCi/μl) per 20 μl reaction mixture. The DNA template was removed using TURBO-DNase. RNA was extracted with hot phenol, precipitated and dissolved in ultrapure water.

Electrophoretic mobility shift assay (EMSA)

For gel-shift assays, 20 μl of a reconstituted ARNP sample containing internally labeled mini-*rplU* transcript and Tc (see below) was mixed with 2 μl of loading buffer (0.05× TBE, 50% glycerol, 0.1% bromophenol blue, 1.5 μg/ml Tc) and loaded onto a 2 mm thick, 10% native polyacrylamide (PAA)-gel (10% PAA, 0.25× TBE, 10 mM MgCl$_2$, 1.5 μg/ml Tc). The gel was pre-run for 1 h at 100 V and 4°C, and the electrophoretic separation was conducted for 3 h at 150 V and 4°C. After gel drying, signals were detected by phosphorimaging using a Bio-Rad molecular imager.

mRNA half-life determination

Rf (inhibitor of transcription initiation) was dissolved in methanol (150 mg/ml) and added to a final concentration of 800 μg/ml to bacterial cultures. Culture aliquots were withdrawn at time points 0, 2, 4, 6 and 8 min and RNA was isolated. To determine the relative levels of specific mRNAs, qRT-PCR analysis with 16S rRNA as a reference was performed (see above). Linear-log graphs were used for half-life calculation.

Coimmunoprecipitation with 3×FLAG-peTrpL

For CoIP with the tagged peptide 3×FLAG-peTrpL, *S. meliloti* 2011 pSRKGm-3×FLAG-peTrpL was used. For control CoIPs, pSRKGm-peTrpL (mock) or pSRKGm-3×FLAG were used instead. Ten minutes after addition of IPTG and one of the antibiotics Tc, Em, Cl, Km or Rf (applied at the above specified subinhibitory concentrations) to a culture, 90 ml cells were harvested by centrifugation at 4°C and 6,000 rpm. The cells were resuspended in 5 ml buffer A (20 mM Tris–HCl, pH 7.5, 150 mM KCl, 1 mM MgCl$_2$, 1 mM DTT) containing 10 mg/ml lysozyme, the respective antibiotic, and protease inhibitor cocktail (Sigma-Aldrich) and lysed by sonication. The cleared lysate was incubated for 2 h with 40 μl Anti-FLAG M2 Magnetic Beads (Sigma-Aldrich) at 4°C. One half of the beads was washed three times with 500 μl buffer A containing 2 μg/ml Tc, while the second half was washed with buffer without Tc (protease inhibitors were used in the first two washing steps). Then the beads were resuspended in 50 μl buffer A (elution fraction) and used for RNA purification with hot-phenol.

MS2-rnTrpL affinity purification

For MS2-MBP (MS2 phage coat protein fused to maltose-binding protein) affinity chromatography (32), *S. meliloti* 2011 pRK-MS2-rnTrpL was used. Mock purification was performed with strain 2011 pRK-MS2, in which the MS2

aptamer was transcribed instead of MS2-rnTrpL. Cells from 90 ml culture of OD 0.5 were washed in 20 ml cold PBS (140 mM NaCl, 3 mM KCl, 10 mM Na_2HPO_4, 2 mM KH_2PO_4, pH 7.4), resuspended in 600 μl buffer B (20 mM Tris, pH 8.0, 150 mM KCl, 1 mM $MgCl_2$, 1 mM DTT) and sonicated. The cleared lysate (350 μl) was applied onto a column of amylose beads, which were non-covalently bound to the MS2-MBP fusion protein (32). To prepare the column, 2 ml Bio-spin disposable chromatography column (Bio-Rad), 70 μl amylose bead suspension (New England Biolabs) and purified MS2-MBP (300 pmol protein in 1 ml buffer B) were used. The column material was incubated for 5 min at 4°C with the lysate, before the flow-through was collected and applied again onto the column. Then the beads were split into two portions, and one of them was washed 3× with 2 ml buffer B containing 2 μg/ml Tc, while the second one was washed with the buffer without Tc. For elution, the beads were resuspended in 250 μl buffer B containing 12 mM maltose. The elution step was repeated. RNA from the resulting elution fractions was purified with hot-phenol. The organic phase of the hot-phenol extracted sample was mixed with 1.5 ml ice-cold acetone and the proteins were precipitated over night at −20°C.

Northern blot analysis

After purification of reconstituted ARNPs by CoIP or MS2-MBP chromatography, resuspended beads were loaded on 10% polyacrylamide-urea gels. Electrophoresis was conducted at 300 V for 3 h and RNA was transferred by semi-dry electroblotting to a positively charged nylon membrane and crosslinked by UV. Radioactive, 5′-labeled oligonucleotide probes were used for hybridization (Supplementary Table S2). For labelling, 15 μCi [γ-^{32}P]-ATP (Hartmann Analytics, Braunschweig, Germany) and 5 U T4 polynucleotide kinase were used in a 10 μl reaction mixture. After incubation for 60 min at 37°C, 30 μl water were added and unincorporated nucleotides were removed using MicroSpin G-25 columns (GE Healthcare Life Sciences). Prehybridization was conducted fort 2 h at 56°C with a buffer containing 6× SSC, 2.5 × Denhardt's solution, 1% SDS and 10 μg/ml salmon sperm DNA. Hybridization was conducted in a solution containing 6 × SSC, 1% SDS, 10 μg/ml salmon sperm DNA for at least 6 h at 56°C. The membrane was washed twice for 2–5 min in 0.01% SDS, 5× SSC at room temperature. Detection and quantification of the signals was performed using a Bio-Rad molecular imager and Quantity One software.

SDS-PAGE and western blot analysis

Proteins were analyzed by SDS-PAGE as described (28,33). Western blot detection of 3×FLAG-peTrpL was conducted as follows (34): The used separating gel of the Tricine-SDS-PAGE contained 16% polyacrylamide (acrylamide:bis-acrylamide 19:1) and 8% glycerol. After electrophoresis in a hand-cast mini-gel (60 V until the sample entered the separating gel followed by 100 V for 3 h), electroblotting onto a PVDF membrane was conducted (0–4 mA per cm^2 for 16 – 24 h at room temperature). The membrane was incubated in blocking solution (2.5 g powdered milk in 50 ml 1× PBS

containing 0.1% Tween 20) for 1 h. After 3× washing for 10 min in PBS containing 0.1% Tween 20, the membrane was incubated for 1.5 h with the monoclonal anti-FLAG M2-peroxidase (HRP) antibody (Sigma-Aldrich), which was diluted 1:1000 in 1× PBS containing 0.1% Tween 20 and 3% bovine serum albumin. After 3× washing for 10 min in PBS containing 0.1% Tween 20, the Lumi-Light Western Blotting Substrate Kit (Roche) was used to detect the signals in a Chemiluminescence Reader (PEQLAB).

Mass spectrometry

Digestion of proteins in a gel slice stained with Coomassie Brilliant Blue was performed as reported elsewhere (35). Gel pieces were covered with ultra-pure water and incubated 15 min in an ultrasonic water bath to recover the peptides, which were then loaded on an EASY-nLC II system (Thermo Fisher Scientific) equipped with an in-house built 20 cm column (inner diameter 100 μm, outer diameter 360 μm) filled with ReproSil-Pur 120 C18-AQ reversed-phase material (3 μm particles, Dr Maisch GmbH). Peptides were eluted with a nonlinear 80 min gradient from 1 to 99% (v/v) solvent B (0.1% (v/v) acetic acid in acetonitrile) with a flow rate of 300 nl/min and injected online into a LTQ Orbitrap XL (Thermo Fisher Scientific). As described in (18), the survey scan at a resolution of $R = 30\,000$ and 1×10^6 automatic gain control target in the Orbitrap with activated lock mass correction was followed by selection of the five most abundant precursor ions for fragmentation. Singly charged ions as well as ions without detected charge states were excluded from MS/MS analyses. For identification of peptides from MS-spectra, a database search was performed with Sorcerer-SEQUEST (4.0.4 build, Sage-N Research) using the Sequest algorithm against a target-decoy integrated proteogenomic database (iPtgxDB; https://iptgxdb.expasy.org/) of *S. meliloti* 2011, which also contained sequences of common laboratory contaminants and FLAG-tagged peTrpL (total entries: 320 482).

The quantification of peTrpL abundance by targeted MS was described before (18). Protein extracts were diluted in 50 mM TEAB (triethylammonium bicarbonate) buffer, pH 8.0 (Sigma-Aldrich) to a final concentration of 0.5 μg/μl. Proteins were reduced (2.5 mM TCEP, Tris-(2-carboxyethyl) phosphine hydrochloride, Invitrogen) at 65°C for 45 min and thiols were alkylated in 5 mM iodacetamide (Sigma-Aldrich) for 15 min at 25°C in the dark. Trypsin (Promega) was added in an enzyme-to-substrate ratio of 1:100 and after 14 h at 37°C, protein digestion was terminated by adding concentrated HCl to a final concentration of 600 mM. Peptides were purified using C18 Zip tips (Pierce). Prior to measurement, samples were spiked with synthetic peptides containing an isotopically labeled amino acid (JPT Peptide Technologies and Thermo Fisher Scientific) to a final concentration of 50 fmol/μl (FLAG-peTrpL), 100 fmol/μl (peTrpL-M) and 1000 fmol/μl (WT-peTrpL). For quantification of peTrpL abundance, the heavy synthetic peptide was used to optimize MS-parameters to achieve the highest sensitivity. The samples were loaded on an EASY-nLC 1000 or an EASY-nLC II system (Thermo Fisher Scientific) equipped with an in-house built 20 cm column as explained above. Peptides

were eluted with a nonlinear gradient from 1 to 99% (v/v) solvent B (0.1% (v/v) acetic acid in acetonitrile) with a flow rate of 300 nl/min and injected online into a TSQ Vantage (Thermo Fisher Scientific). The selectivity for both Q1 and Q3 were set to 0.7 Da (FWHM). SRM mode applying a collision gas pressure of 1.2 mTorr in Q2 was used. All raw files from targeted MS were processed using Skyline 4.2 (36). A peptide ratio of native and heavy peTrpL peptide was based on five transitions. Peptide ratios of three biological replicates were averaged if their dot product was >0.7. The concentration of peTrpL in the sample was calculated based on the peptide ratios and the added amount of heavy peptide.

ARNP reconstitution

Peptides were synthesized by Thermo Fisher Scientific. For ARNP reconstitution, *in vitro* transcribed MS2-rnTrpL (100 ng; 2 pmol) and mini-*rplU* (100 ng; 4.4 pmol), WT peTrpL (100 ng, 22 pmol), and Tc (final concentration of 2 μg/ml) were mixed in buffer A, in a final volume of 50 μl. When Tc was omitted, the same volume of the solvent ethanol was added. The samples were incubated for 20 min at 20°C under shaking. Optionally, half of WT peTrpL was replaced by the tagged peptide; *in vitro* transcribed rn-TrpL was used instead of the MS2-rnTrpL transcript; Tc was replaced by another antibiotic used at the subinhibitory concentration specified above; mutated *in vitro* transcripts were used; 100 ng as-rnTrpL or 100 ng as-*rplU* or both together were additionally added; 100 or 500 ng of unrelated 70 nt *smeR2 in vitro* transcript was additionally added. MS2-rnTrpL or 3× FLAG-peTrpL containing reconstituted ARNPs were isolated by MS2-MBP chromatography or CoIP as described above using 20 μl beads. The washing steps were performed with 100 μl buffer, the washed beads were resuspended in 50 μl (elution) buffer and 5 μl of the resuspended beads were mixed with formamide-urea loading buffer, heated at 65°C and loaded on denaturing polyacrylamide gel for northern blot analysis. Reconstituted ARNPs containing non-tagged components and internally labeled mini-*rplU* transcript were analyzed by EMSA (5 μl of each reconstitution sample were loaded on a gel).

Additionally, native and reconstituted ARNPs were subjected to disassembly by diluting the sample with a buffer, which did not contain antibiotic, and reassembly was achieved by raising the antibiotic concentration. MS2-MBP purified *rplUrpmA*-ARNP was portioned in samples containing approximately 300 ng endogenous RNA (mainly *rplUrpmA* mRNA, rnTrpL and corresponding asRNAs). For competition experiments, 1:1 mixture of mini-*trpD* and mini-*rplU in vitro* transcripts (300 ng of each transcript) was added to such samples, which were then used for ARNP disassembly and reassembly.

Computational analysis

Two hundred and eighty-one genomes of Rhizobiales were downloaded from GenBank (37) in August 2018 and analyzed for presence of ORFs located upstream of *trpE* and at least two consecutive UGG codons. Sequence logos were constructed using WebLogo (38). RNA-RNA interactions and secondary structures were predicted by IntaRNA and MFOLD, respectively (39,40).

RESULTS

The *trp* attenuator responds to tetracycline exposure

We hypothesized that transient ribosome stalling at the 5′-end of *trpL* in the nascent RNA would lead to transcription attenuation and rnTrpL sRNA liberation in *S. meliloti*. To test this, it was necessary to distinguish transcription attenuation due to Trp availability from possible attenuation due to exposure to Tc. In the prototrophic strain *S. meliloti* 2011, the rnTrpL sRNA is present during growth in rich TY and GMX minimal media, because even in minimal medium, due to expression of *trp* genes, there are sufficient Trp-charged tRNAs to cause transcription attenuation (Supplementary Figure S1). Therefore, we used a *ΔtrpC* mutant of strain 2011, in which relief of transcription attenuation (cotranscription of *trpL* with *trpE(G)*) occurs under Trp limiting conditions (13,14).

After 4 h of growth under Trp limiting (Low Trp) conditions (minimal medium containing 2 μg/ml Trp), rnTrpL was not detectable by northern hybridization (lane 2 in Figure 2B). Addition of Tc to a final concentration of 1.5 μg/ml (below the minimal inhibitory concentration of 2 μg/ml) resulted in rnTrpL accumulation (Figure 2B, lanes 3 and 4), in line with the proposed transcription attenuation in response to impairment of translation initiation. After removal of Tc from the medium, the rnTrpL level decreased again (compare lanes 4 and 5 in Figure 2B). Additionally, we analyzed by qRT-PCR the relative levels of 5′-leader, *trpL*- and *trpE(G)*-containing cotranscript, and *trpE(G)* mRNA. The results confirmed that the observed changes in the rnTrpL level (Figure 2B) are due to transcription attenuation and its relief (Supplementary Figure S2). Thus, the *trp* attenuator responds to Tc exposure by sRNA liberation.

Recently we found that in *S. meliloti* 2011 cultures grown in rich TY medium, the level of peTrpL is strongly increased upon Tc exposure (18). Here, mass spectrometry (MS) was used to analyze the peTrpL level in minimal medium and strong accumulation was detected 10 min after addition of 1.5 μg/ml Tc to the cultures (Figure 2C). Under Low Trp conditions without Tc, no peTrpL could be detected, most probably because it was below the limit of detection by targeted MS (<0.1 fmol peTrpL/μl sample as obtained from calibration curves using the pure peptide). Given the fact that peTrpL was well detectable under Low Trp conditions with Tc (Figure 2C), we assume a strong accumulation of peTrpL in presence of Tc. Under High Trp conditions (20 μg/ml Trp), peTrpL was detectable in the samples without Tc, suggesting generally higher abundance of peTrpL under High Trp conditions compared to low Trp conditions. Moreover, peTrpL accumulated on average >300-fold when Tc was added to High Trp samples (Figure 2C).

In summary, the available data (Figure 2, Supplementary Figure S1) and (12,18) show that in minimal and in rich medium, the *trans*-acting products of the *trp* attenuator, the leader peptide peTrpL and the sRNA rnTrpL, are present and/or accumulate under conditions of Tc exposure. In the following, we provide evidence for a joint, Tc-dependent function of peTrpL and rnTrpL in the regulation of *rplUrpmA*. If not indicated otherwise, cultures grown in rich TY medium were used.
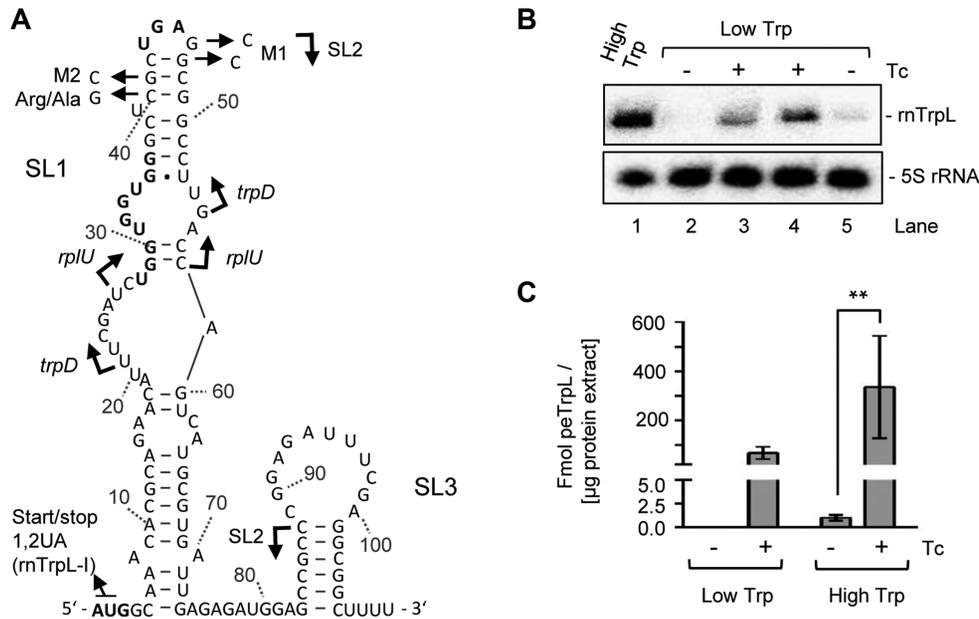
Figure 2. The *S. meliloti trp* attenuator responds to tetracycline exposure. (**A**) Secondary structure of rnTrpL (as experimentally determined in (14)) with indicated SL1, SL3, and mutations used in this work (M1, M2). The sequence corresponding to SL2 as well as the beginning and end of rnTrpL regions predicted to base pair with *trpD* and *rplU*, respectively, are indicated with correspondingly marked, flexed arrows. Start, stop and Trp codons of the *trpL* ORF are in bold. (**B**) Phosphorimage showing northern blot analysis of strain 2011 *ΔtrpC* grown in GMX minimal medium with 20 μg/ml Trp (High Trp conditions) or 2 μg/ml Trp (Low Trp conditions). Presence of 1.5 μg/ml Tc is indicated (−Tc, corresponding volume of the solvent ethanol was added). Lane 1: RNA from a culture grown in High Trp medium to OD_{600} of 0.5; lane 2: RNA from the same culture after dilution in Low Trp medium and 4 h growth to OD_{600} of 0.5; lanes 3 and 4: Tc was added to the lane 2 culture and RNA was purified 10 and 20 min thereafter; lane 5: cells of the lane 4 culture were washed in Low Trp-medium without Tc, incubated for 10 min, and used for RNA isolation. 30 μg total RNA was loaded in each lane, except for lane 1 in which 10 μg RNA was loaded. First, a probe directed against rnTrpL was used and then the membrane was re-hybridized with the 5S rRNA-specific probe (loading control). Detected RNAs are indicated. For qRT-PCR analysis of the RNA samples, see Supplementary Figure S2. (**C**) Results of targeted MS of peTrpL abundance under Low and High Trp conditions in GMX minimal medium with and without Tc in strain 2011. Error bars represent the standard deviations obtained from three biological replicates. In the Low Trp, -Tc samples, no peTrpL could be detected. According to the Student's t-test: **: *P*-value ≤ 0.01.

rnTrpL, peTrpL and Tc are needed for posttranscriptional *rplUrpmA* regulation

To address the predicted interaction between rnTrpL and *rplUrpmA* mRNA (12), we used plasmid pSRKTc-rnTrpL (Figure 3A), which provides resistance to Tc and allows for IPTG-inducible production of a rnTrpL variant named lacZ'-rnTrpL (and simultaneous production of peTrpL encoded by the sRNA). While rnTrpL directly starts with the ATG of *trpL* (Figure 2B), lacZ'-rnTrpL harbors the 5'-UTR of *lacZ* (see corresponding plasmid scheme in Figure 3A). In a previous study, we could show that lacZ'-rnTrpL is functional and destabilizes *trpDC* mRNA (14). The lacZ'-rnTrpL transcription was induced for 10 min in *S. meliloti* 2011 *ΔtrpL*, in which the rnTrpL sequence and thus also the *trpL* ORF were deleted from the chromosome. Using qRT-PCR, we detected an almost fourfold decrease in the *rpmA* mRNA level (see the first two bars in Figure 3B), suggesting a possible role of rnTrpL and/or peTrpL in downregulation of *rplUrpmA*.

Next, we provided the peptide and sRNA functions on different plasmids. The Tc resistance plasmid pRK-rnTrpL-I, from which a sRNA derivative with inactivated *trpL* ORF is constitutively transcribed (rnTrpL-I harbors a start to stop codon mutation, see Figure 2A), and the gentamycin (Gm) resistance plasmid pSRKGm-peTrpL, which allows for IPTG-inducible peTrpL production (Figure 3A), were

used separately or together in strain 2011 *ΔtrpL*. Using qRT-PCR, we determined changes in the level of *rplUrpmA* mRNA 10 min after IPTG addition (Figure 3B). Surprisingly, we found that the *rplUrpmA* mRNA level was decreased only if both the sRNA and the peptide were produced (Figure 3B). In contrast, production of the rnTrpL-I only was sufficient for *trpC* mRNA decrease (representing the *trpDC* target of rnTrpL), while the level of *trpE* mRNA, which is not a target of rnTrpL in *trans*, was not changed (Figure 3B, red and orange bars). These results suggest that, in contrast to *trpDC*, *rplUrpmA* is a peTrpL-dependent target of the sRNA rnTrpL.

We also tested whether induced peTrpL overproduction will influence *rplUrpmA* in a Tc dependent manner in strain 2011 producing native rnTrpL and peTrpL from the chromosome. When 2011 pSRKGm-peTrpL cultures grown in the presence of gentamycin (Gm) were used, no change in the *rpmA* mRNA level was observed 10 min after IPTG addition (Figure 3C). In contrast, in a two-plasmid strain, which contained in addition the pRK4352 empty plasmid and was cultivated in medium with Gm and Tc, the *rpmA* mRNA level was decreased after IPTG addition (Figure 3C). The pRK4352 containing strain was cultured in medium with 20 μg/ml Tc, and the Tc-specific TetA efflux pump encoded by the plasmid provided resistance to Tc. Our previous data suggested that Tc is present in the cells of
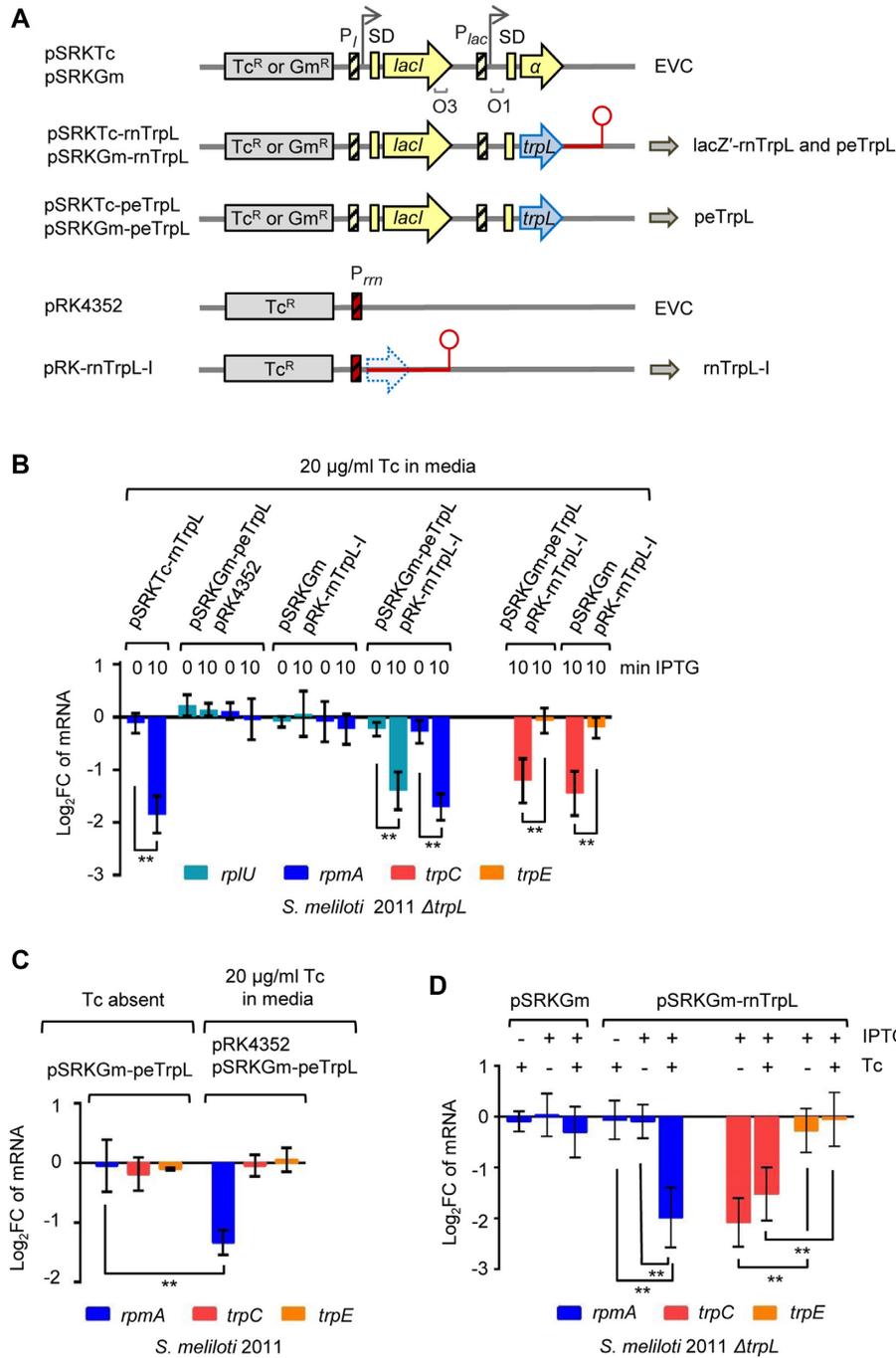
Figure 3. rnTrpL, peTrpL and Tc are needed for downregulation of *rplUrpmA*. (**A**) Used plasmids and their products. The pSRKTc and pSRKGm plasmids confer resistance to Tc and Gm, respectively. They contain a *lac*-module from *E. coli* (in yellow), which ensures tight repression of cloned genes and their induction by IPTG. It comprises the *lacI* gene (harboring the operator O_3) with its promoter P_I, the intergenic region between *lacI* and *lacZ*, the P_{lac} promoter, the operator O_1, which is located in the 5′-UTR of *lacZ*, and an engineered *lacZ*α containing a multiple cloning site (30). Shine-Dalgarno sequences (SD) are indicated by small, non-hatched rectangles. The start codon of *lacZ*α is a part of an NdeI restriction site, which was used to clone either rnTrpL (which is leaderless and starts with ATG of *trpL*) or recombinant *trpL* ORF containing synonymous codons (14). The pRK4352 plasmid contains a heterologous *rrn* promoter (29) and was used to produce the sRNA-derivative rnTrpL-I with inactive *trpL* ORF. EVC, empty vector control. Relevant genes are depicted by internally labeled arrows. For other descriptions see Figure 1. (B–D), results of qRT-PCR analyses. Shown are log₂-transformed fold changes (log₂FC) in the levels of the indicated mRNAs. Used strains and plasmids are given. Bacteria were cultivated in rich TY medium and presence of Tc is indicated. (**B**) RNA from *S. meliloti* 2011 *ΔtrpL* strains harboring the indicated plasmids was compared to that of the corresponding EVC before (0 min) and 10 min after IPTG addition. (**C**) RNA isolated 10 min after IPTG addition was compared to RNA isolated at the time point 0. (**D**) RNA isolated 10 min after addition of IPTG and/or 1.5 μg/ml Tc was compared to RNA isolated at the time point 0. Importantly, decrease in the *rpmA* mRNA level was not detected in the EVC cultures harboring pSRKGm. Each graph shows means and standard deviations from three independent experiments. According to the Student's *t*-test: *P-value ≤ 0.05; **P-value ≤ 0.01.

such cultures at a certain level (18). Thus, one possible explanation of the Figure 3C result is that the overexpressed peTrpL directs the native rnTrpL sRNA to *rplUrpmA*, and that for this Tc is needed.

To test whether Tc is needed for *rplUrpmA* downregulation by rnTrpL and peTrpL, we used *S. meliloti* 2011 *ΔtrpL* harboring the Gm-resistance plasmid pSRKGm-rnTrpL, which allows for IPTG-inducible production of lacZ′-rnTrpL and peTrpL (Figure 3A). Cultures of this strain were supplemented with either IPTG or Tc (1.5 μg/ml), or with both IPTG and Tc, and changes in mRNA levels were subsequently measured by qRT-PCR. The level of *rpmA* mRNA was decreased only in cultures supplemented with both IPTG and Tc (Figure 3D). Such a decrease was not observed in the empty vector control strain (EVC) containing pSRKGm. Furthermore, in the pSRKGm-rnTrpL containing strain, the level of *trpC* mRNA was decreased after IPTG addition even without Tc, and that of the control *trpE* mRNA was not changed significantly under all conditions (Figure 3D). These results suggest that rnTrpL and peTrpL act in conjunction with Tc in the regulation of *rplUrpmA*.

Moreover, we exposed cultures of the Tc-sensitive strains 2011 and 2011 *ΔtrpL* (without recombinant plasmids) to 1.5 μg/ml Tc for 10 min and analyzed changes in the level of *rplUrpmA* mRNA by qRT-PCR (Figure 4A and B). Upon Tc exposure, the *rplUrpmA* mRNA level was decreased in strain 2011 but not in the deletion mutant. The Tc-triggered, *trpL*-dependent decrease was not observed for the control mRNAs *trpC* and *trpE* (Figure 4B). The same qRT-PCR data was used to compare the parental strain 2011 to the *ΔtrpL* mutant (Figure 4A and C). Without Tc exposure, the *rplUrpmA* mRNA level in both strains was similar, and, as expected, the *trpC* mRNA level in the parental strain was lower than that in the mutant. Upon Tc exposure, however, the *rplUrpmA* level in the parental strain was lower than that in the mutant. Interestingly, under Tc exposure conditions the difference in the *trpC* mRNA level of both strains was smaller than in the absence of Tc (Figure 4C). This suggests that in the presence of Tc, the rnTrpL sRNA is engaged in regulation of *rplUrpmA* rather than in regulation of *trpDC*.

Next, we tested whether other translation initiation inhibiting antibiotics such as erythromycin (Em), chloramphenicol (Cl) and kanamycin (Km) also trigger a *trpL*-dependent *rplUrpmA* downregulation. As a negative control, the inhibitor of transcription initiation rifampicin (Rf) was used. The antibiotics were added at subinhibitory concentrations to cultures of strains 2011 and 2011 *ΔtrpL* (without recombinant plasmids)*, and mRNA changes were analyzed by qRT-PCR. In strain 2011, the *rpmA* mRNA level was decreased when Em, Cl or Km were applied, but not upon addition of Rf (Figure 4D). In contrast, a significant *rpm*A decrease was not detected in strain 2011 *ΔtrpL,* supporting the critical role of the *trans*-acting products of the *trp* attenuator in *rplUrpmA* downregulation upon exposure to translation inhibitors.

The sRNA rnTrpL base pairs with *rplU* mRNA

To learn more about the role of rnTrpL in *rplUrpmA* downregulation, the predicted base pairing between rnTrpL and *rplU* in *rplUrpmA* mRNA was studied *in vivo*. For this, two-plasmid assays were performed in the 2011 *ΔtrpL* mutant. Each tested strain contained either the Tc-resistance empty plasmid pSRKTc (Figure 3A), or one of its derivatives for production of lacZ′-rnTrpL sRNA or mutated sRNAs with weaker predicted base pairing to *rplU* (Figure 5A and B). Previously, it was shown that these mutations do not influence the level of the ectopically produced sRNAs (14). While the M1 mutation is located downstream of the *trpL* ORF, the M2 mutation leads to an R to A replacement in peTrpL (Figures 2A and 5B), which is produced along with the sRNA upon induction with IPTG. Additionally, each strain contained a second, pSRKGm-based plasmid with a bicistronic *rplUrpmA′::egfp* reporter fusion or one of its derivatives with compensatory mutations restoring the sRNA-mRNA base pairing (Figure 5A and B). Cultures were grown in medium with Gm and Tc, the sRNA and reporter constructs were co-induced with IPTG for 20 min, and fluorescence was measured.

Fluorescence of the fusion protein L27′-EGFP derived from the *rplUrpmA′::egfp* construct was strongly decreased if lacZ′-rnTrpL was co-expressed (Figure 5C), in line with the idea that the sRNA binds to *rplU* and thereby induces a reduction of *rplUrpmA′::egfp* mRNA levels. In contrast, sRNA derivatives harboring the M1 and M2 mutations, respectively, did not cause this effect. Importantly, the compensatory mutations in the *rplUrpmA′::egfp* transcript, which were designed to restore the base pairing to the mutated sRNAs (Figure 5B), specifically restored the negative effect of the sRNA on fluorescence (Figure 5C). These results validate the base pairing between rnTrpL and *rplU* and show that even subtle changes in the base pairing interactions may have a major impact on the downregulation of *rplUrpmA*.

The sRNA rnTrpL destabilizes *rplUrpmA* mRNA

The Tc- and peTrpL-dependent *rplUrpmA* downregulation by rnTrpL could be explained by *rplUrpmA* destabilization. To test this, 2011 *ΔtrpL,*pSRKGm-rnTrpL cultures were used, in which the lacZ′-rnTrpL transcription (and thus concomitant peTrpL production) was induced by IPTG. In parallel, cultures were analyzed, to which IPTG and 1.5 μg/ml Tc were added. Ten minutes after induction, Rf was added to stop initiation of cellular transcription. Samples were withdrawn at several time points after Rf addition and decay of *rplUrpmA* mRNA in time was analyzed by qRT-PCR. The half-life of *rplUrpmA* was significantly shortened only in cultures to which IPTG and Tc were added (Figure 6A, Supplementary Figure S3).

Furthermore, we also tested whether the *rplUrpmA* mRNA is destabilized in cultures of strains 2011 and 2011 *ΔtrpL* (without plasmids) after addition of 1.5 μg/ml Tc. In line with the above results, upon Tc exposure, the *rplUrpmA* mRNA stability was decreased in the parental strain but not in the *ΔtrpL* mutant (Figure 6B and Supplementary Figure S3). Altogether, the above results show that, in the presence of peTrpL, the sRNA rnTrpL base pairs with *rplU* and destabilizes *rplUrpmA* mRNA in a Tc-dependent manner.
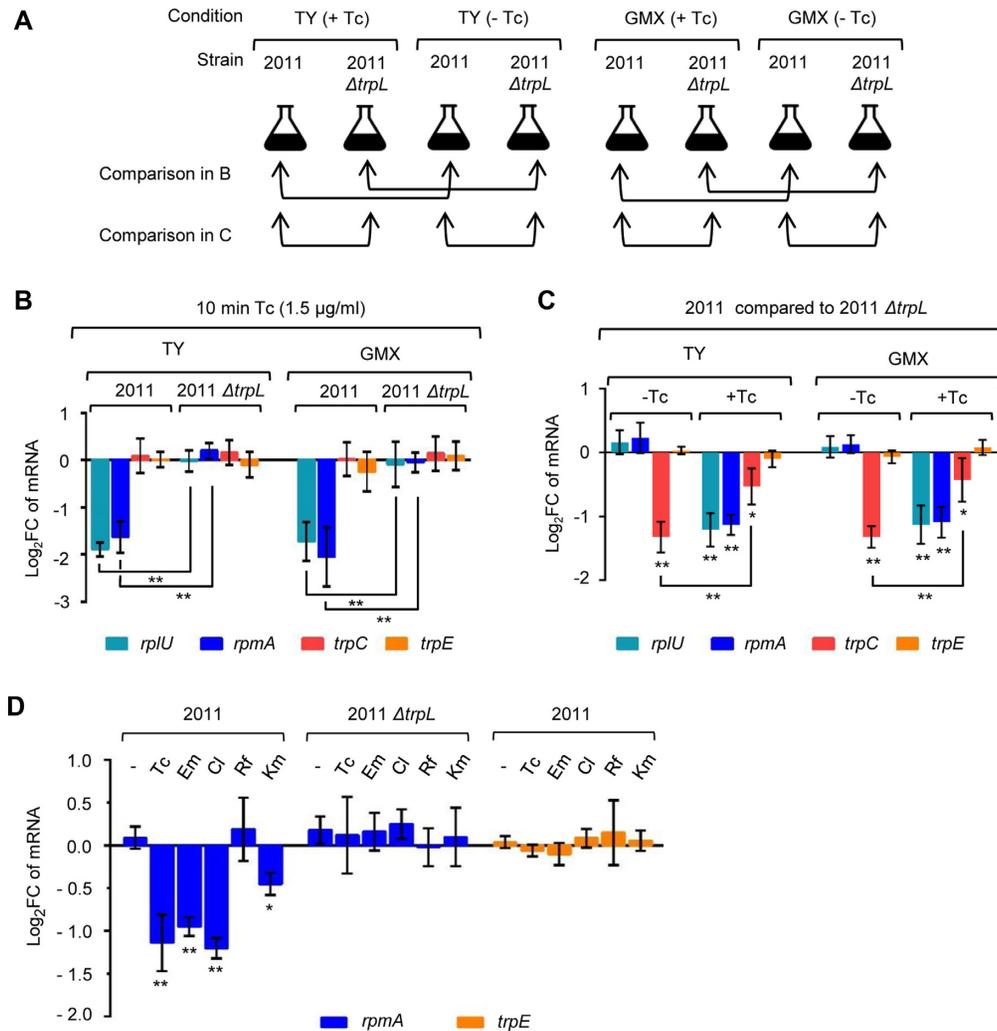
Figure 4. Comparison of the parental strain 2011 and the *ΔtrpL* mutant supports *trpL*-dependent downregulation of *rplUrpmA* upon exposure to Tc and several inhibitors of translation initiation. Shown are log₂FC in the levels of the indicated mRNAs as determined by qRT-PCR. Used strains are given. The indicated antibiotics were applied at subinhibitory concentrations. (**A**) Scheme of the experiment leading to the results shown in (**B**) and (**C**). Relative mRNA levels were determined by qRT-PCR. The same set of qRT-PCR data was used to compare the mRNA levels in a strain under different conditions (**B**) or the mRNA levels of the two strains (**C**). (**B**) RNA isolated from cultures exposed for 10 min to 1.5 µg/ml Tc (+Tc) was compared to RNA isolated from cultures to which the solvent ethanol was added (–Tc). Cultures were grown either in rich TY medium or in GMX minimal medium (indicated). (**C**) RNA isolated from strain 2011 was compared to RNA isolated form the 2011 *ΔtrpL* mutant. The used growth medium and the presence or absence of Tc is indicated. (**D**) RNA isolated from TY cultures exposed for 10 min to the indicated antibiotics was compared to RNA isolated from TY cultures to which the respective antibiotic solvent was added. Each graph shows means and standard deviations from three independent experiments. According to the Student's *t*-test: *P-value ≤ 0.05; **P-value ≤ 0.01.

rnTrpL and peTrpL are in an ARNP complex with *rplUrpmA* mRNA and antisense RNA

The above data suggest that rnTrpL, peTrpL, *rplUrpmA* mRNA and Tc form a complex in *S. meliloti*, similar to the recently described *smeR*-ARNP containing peTrpL, *smeR* mRNA, as-*smeR* RNA and Tc (18). We took advantage of existing RNA-Seq data of RNA that was coimmunoprecipitated with a 3×FLAG-peTrpL peptide from *S. meliloti* (18) (https://www.ncbi.nlm.nih.gov/geo/query/acc.cgi?acc=GSE118689) and found that in addition to *smeR* and as-*smeR* RNA, only rnTrpL, *rplUrpmA* and corresponding asRNAs were enriched by the coimmunoprecipitation (CoIP). qRT-PCR analysis confirmed the specific and Tc-dependent CoIP of these RNAs: rnTrpL, *rplUrpmA*

mRNA and their asRNAs were coimmunoprecipitated with 3×FLAG-peTrpL only if Tc was present in the growth medium and a buffer containing Tc was used in the washing steps of the CoIP procedure (Supplementary Figure S4). Importantly, such an enrichment was not achieved in a CoIP with a control 3×FLAG peptide (Supplementary Figure S4). The coimmunoprecipitated complex was designated *rplUrpmA*-ARNP.

Of note, the CoIP with 3×FLAG-peTrpL was conducted using strain 2011, because induction of the 3×FLAG-peTrpL peptide decreased the *rplUrpmA* mRNA level only in wild type but not in *ΔtrpL* background (Supplementary Figure S5). This suggested that not only in the *smeR*-ARNP (18), but also in the *rplUrpmA*-ARNP, the 3×FLAG-
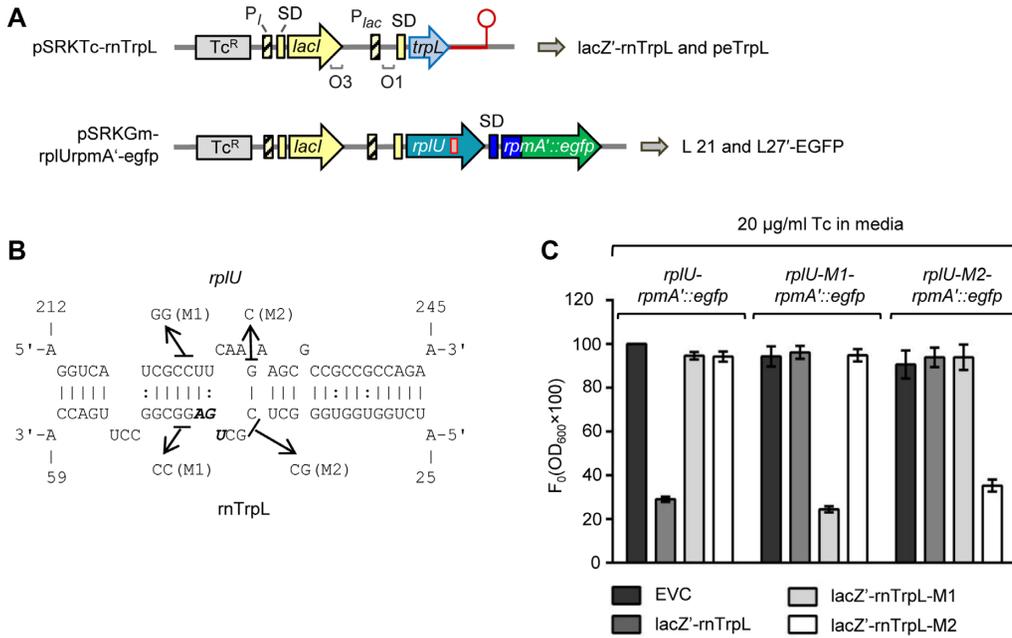
Figure 5. rnTrpL base pairs with *rplU* and downregulates *rplUrpmA*. (**A**) Scheme of the used plasmids. The binding site of rnTrpL in *rplU* is indicated by a red rectangle. For other descriptions see Figure 3A. (**B**) Scheme of the duplex structure predicted to be formed between *rplU* and rnTrpL ($\Delta G = -11.54$ kcal/mol). The used mutations in lacZ'-rnTrpL and compensatory mutations in *rplU* are given. (**C**) Analysis of possible base pairing interactions between lacZ'-rnTrpL and the fusion mRNA *rplUrpmA'::egfp* in strain 2011 *ΔtrpL*. Used constructs and mutations are indicated. Bacteria were cultivated in rich TY medium. The fluorescence of the strain expressing *rplU-rpmA'::egfp* from plasmid pSRKGm-rplUrpmA'-egfp and containing the empty vector pSRKTc, which was used for sRNA production in the other strains, was set to 100%. Shown are means and standard deviations of three independent experiments.
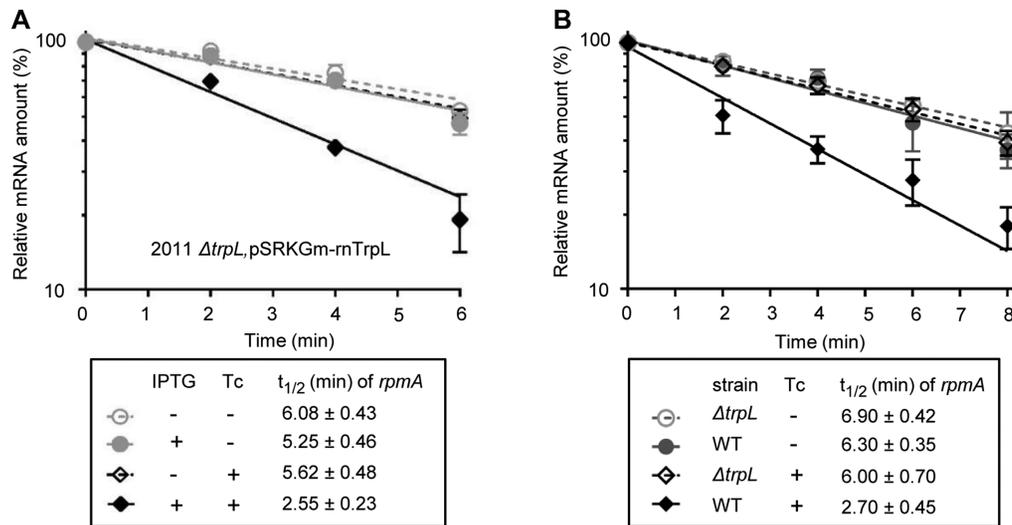
Figure 6. The sRNA rnTrpL destabilizes *rplUrpmA* in a Tc-dependent manner. (**A**) Influence of sRNA overproduction and/or Tc addition on the half-life of *rpmA* mRNA. To *S. meliloti* 2011 *ΔtrpL*,pSRKGm-rnTrpL cultures grown in rich TY medium, Tc (1.5 µg/ml) and/or IPTG inducing lacZ'-rnTrpL (and thus also peTrpL) production were added. After 10 min, rifampicin (Rf) was added to stop initiation of cellular transcription and aliquots were withdrawn for RNA isolation at the indicated time points. Relative RNA levels were determined by qRT-PCR. The calculated half-lives are given. For several time points, the standard deviation is smaller than the used symbols. (**B**) Influence of Tc on the *rpmA* mRNA half-life in the parental strain 2011 and the 2011 *ΔtrpL* mutant. 10 min after addition of Tc to the cultures, rifampicin was added. For other descriptions see A). Shown are means and standard deviations of three independent experiments. Half-life determination for *rplU* mRNA and the control mRNA *rpoB* are presented in Supplementary Figure S3.

peTrpL works in a complex with the chromosomally produced wild type peptide.

Next, we tested whether other translation inhibiting antibiotics support the *rplUrpmA*-ARNP. To individual 2011 pSRKGm-3×FLAG-peTrpL cultures, one of the following antibiotics was added at a subinhibitory concentration: Tc (positive control), Rf (negative control), Em, Cl or Km. Simultaneously, IPTG was added to induce 3×FLAG-peTrpL production, and 10 min later, CoIP was conducted. One half of the beads of each CoIP was washed with a buffer containing the respective antibiotic, while the other half was washed with a buffer lacking the antibiotic, and coimmunoprecipitated RNA was analyzed by qRT-PCR in comparison to a mock control. The sRNA rnTrpL, *rplUrpmA* mRNA and the corresponding asRNAs (but not the control mRNA *trpE*) were coimmunoprecipitated in the presence of the translation inhibitors Tc, Em, Cl and Km, but not in the presence of the transcription inhibitor Rf (Figure 7A). This suggests that structurally unrelated translation inhibitors are capable to promote the *rplUrpmA*-ARNP formation.

According to (18) and the above data, two different ARNP complexes coimmunoprecipitate with 3×FLAG-peTrpL in the presence of Tc: a *smeR*- and a *rplUrpmA*-ARNP. While the s*meR*-ARNP does not depend on rnTrpL (18), our data suggest that rnTrpL is a part of the *rplUrpmA*-ARNP. To isolate only the *rplUrpmA*-ARNP, we decided to use a 5′-terminally tagged MS2-rnTrpL sRNA and MS2-MBP affinity chromatography (32). The functionality of the plasmid-borne MS2-rnTrpL in *rplUrpmA* downregulation was confirmed (Supplementary Figure S5). Cultures of strain 2011 pRK-MS2-rnTrpL,pSRKGm-3×FLAG-peTrpL were used, in which MS2-rnTrpL was constitutively transcribed and the 3×FLAG-peTrpL peptide production was induced for 10 min. The tagged peptide (4.5 kDa) was used to detect the presence of peptide in the purified *rplUrpmA*-ARNP complex, because native peTrpL (14 aa, 1.8 kDa) was not detectable by SDS-PAGE.

After purification of the MS2-rnTrpL sRNA together with its interaction partners, the elution fractions were analyzed by Tricine-SDS-PAGE showing that the 3×FLAG-peTrpL peptide was copurified in a Tc-dependent manner (Figure 7B). The identity of the atypically migrating 3×FLAG-peTrpL band was confirmed by Western blot analysis (Supplementary Figure S6) and mass spectrometry (Supplementary Table S3); larger proteins were not detected in the complex (Supplementary Figure S6). Further, *rplUrpmA* mRNA and the corresponding asRNA were copurified in a Tc-dependent manner with MS2-rnTrpL (Figure 7C). Additionally, *trpC* mRNA was copurified in the presence and (even in larger amounts) in the absence of Tc in the washing buffer. Importantly, *trpE* and *smeR* mRNA were not co-purified with MS2-rnTrpL (Figure 7C), supporting the specificity of this approach and demonstrating the successful separation of the *rplUrpmA*-ARNP from the *smeR*-ARNP.

ARNP reconstitution reveals a crucial role of rnTrpL in complex formation

To address the role of peTrpL and Tc in ARNP formation, *in vitro* reconstitution was performed using the following components: (i) 155 nt *in vitro* transcribed MS2-rnTrpL sRNA, (ii) synthetic wild type (WT) peTrpL, (iii) 71 nt *in vitro* transcript comprising the *rplU* region predicted to base pair with rnTrpL (mini-*rplU*, for a predicted secondary structure see Supplementary Figure S7) and (iv) Tc. Reconstituted complexes were purified by MS2-MBP affinity chromatography and analyzed by northern blot hybridization. Mini-*rplU* was copurified with MS2-rnTrpL only if both peTrpL and Tc were present in the reaction mixture (compare the elution fractions in lanes 7, 12 and 19 in Figure 8A). We conclude that the sRNA requires the peptide and the antibiotic for binding to the *rplU* target, and at least *in vitro*, asRNA is not necessary for ARNP formation.

To assess the importance of rnTrpL in ARNP assembly, in the Tc-containing reconstitution reaction non-tagged, *in vitro* transcribed rnTrpL and mini-*rplU* were used, and half of WT peTrpL was replaced by 3×FLAG-peTrpL to enable purification of the reconstituted complexes by CoIP. Only when all components were present in the mixture, mini-*rplU* and rnTrpL were found to coimmunoprecipitate with the tagged peptide (compare the elution fractions in lane 7, 12 and 17 in Figure 8B). This result confirms the importance of rnTrpL for ARNP formation. Moreover, it shows that even in the presence of Tc, the peptide(s) cannot interact with rnTrpL or *rplU* separately. Together, Figure 8A and B shows that four components (sRNA, target mRNA, peptide and Tc) are necessary and sufficient for the *rplU*-ARNP assembly *in vitro*.

To test whether the complementarity between rnTrpL and *rplU* is important for the ARNP assembly, an *in vitro* transcribed rnTrpL-M1 variant and a mini-*rplU*-M1 transcript (for the M1 mutations, see Figure 5B) were used. Reconstituted complexes containing 3×FLAG-peTrpL and WT peTrpL were purified by CoIP. When rnTrpL-M1 was used together with WT mini-*rplU*, very low amount of both transcripts was coimmunoprecipitated with the peptide(s) (compare the elution fractions in Figure 8C, lanes 7 and 12). However, when rnTrpL-M1 was used together with mini-*rplU*-M1 and thus complementation was restored, both transcripts were coimmunoprecipitated efficiently with the peptide(s) (lane 17 in Figure 8C). Thus, the complementarity between the sRNA and the mRNA is crucial for the ARNP formation.

Finally, we tested whether the above used antibiotics support ARNP formation *in vitro*. Reconstitution was conducted using *in vitro* transcribed MS2-rnTrpL, mini-*rplU*, WT peTrpL and Em, Cl, Rf or Km. In line with Figure 7A, the mini-*rplU* transcript was co-purified with MS2-rnTrpL when Em, Cl or Km was used, but not if Rf was used (Figure 8D). Thus, structurally different translation inhibitors can promote the *rplU*-ARNP assembly, for which the sRNA rnTrpL plays a crucial role.
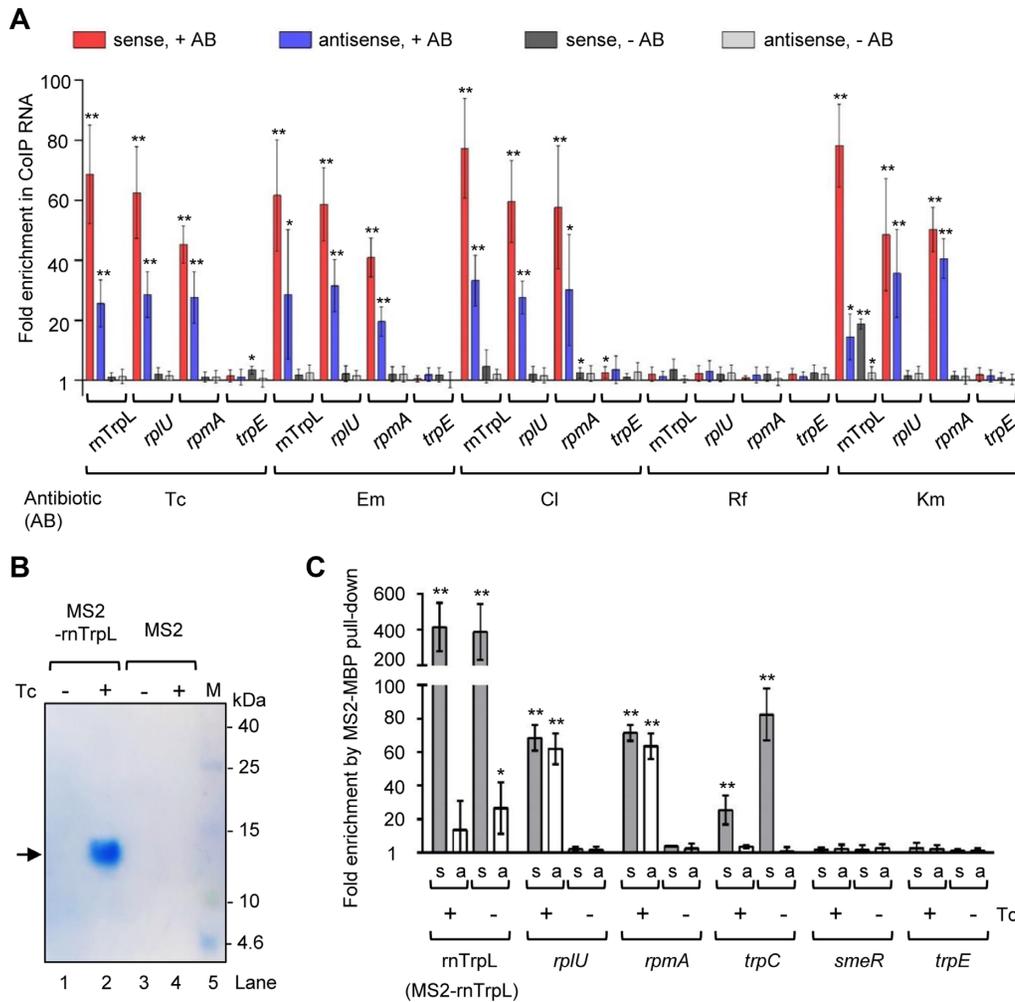
Figure 7. rnTrpL and peTrpL are in an ARNP complex with *rplUrpmA* mRNA and antisense RNA. (**A**) qRT-PCR analysis of rnTrpL and the indicated mRNAs in CoIP samples from strain 2011 pSRKGm-3×FLAG-peTrpL cultivated in rich TY medium. Enrichment was calculated in comparison to the mock CoIP conducted with strain 2011 pSRKGm-peTrpL. CoIP was performed 10 min after addition of IPTG and one of the indicated antibiotics, which was used at a subinhibitory concentration. +AB: the same antibiotic concentration was used in the washing buffer; -AB: washing buffer without antibiotic was used. (**B**) Coomassie stained Tricine-SDS-gel showing co-purification of 3× FLAG-peTrpL with MS2-rnTrpL in the presence of Tc. MS2-rnTrpL: elution samples of MS2-MBP affinity chromatography purification from strain 2011 pSRKGm-3×FLAG-peTrpL,pRK-MS2-rnTrpL. MS2: elution fractions of a control, mock purification from a strain producing the MS2 RNA aptamer instead of MS2-rnTrpL. The affinity chromatography was conducted 10 min after addition of IPTG to the cultures. Presence of Tc in the washing buffer of the chromatography procedure is indicated. Migration of marker protein bands (lane M, in kDa) is indicated. The 3×FLAG-peTrpL band is marked with an arrow. (**C**) qRT-PCR analysis of the indicated RNAs (s: sense RNA; a: asRNA) in elution samples of MS2-MBP affinity chromatography purification from strain 2011 pSRKGm-3×FLAG-peTrpL,pRK-MS2-rnTrpL. Enrichment was calculated in comparison to the mock control. For other descriptions, see B). Shown are means with standard deviations from three independent experiments.

Indication for supportive role of the asRNAs in ARNP formation

Although asRNAs were not necessary for ARNP reconstitution *in vitro* (Figure 8), they were co-purified in the native complexes from *S. meliloti* (Figure 7) and therefore we tested whether they can influence the ARNP assembly. To reconstitution samples containing rnTrpL, 3×FLAG-peTrpL, WT peTrpL, mini-*rplU* and Tc, the antisense transcripts as-rnTrpL or as-*rplU*, or both (1:1 to their sense counterpart) were added. Northern blot analysis of CoIP-purified ARNPs revealed increased complex formation in the presence of the asRNAs. This effect was specific, since addition of an unrelated, 70 nt transcript *smeR2* (18) did not

increase the complex formation (Figure 9A and B). Thus, the asRNAs probably have a supportive role in ARNP formation.

To provide evidence for asRNA transcription in *S. meliloti*, the regions encompassing ∼300 nt upstream of the putative TSS of each asRNA were cloned in promoter fusion plasmids pRS1-P$_{as\text{-}rnTrpL}$ and pRS1-P$_{as\text{-}rplUrpmA}$ (Figure 9C). Each of the plasmids was conjugated into strain 2011 and using qRT-PCR, the level of the reporter *egfp* mRNA was compared to that in the EVC, which contained pRS1-SD-egfp. The used plasmids carried a Gm resistance gene. When no other antibiotic besides Gm was present in the medium, background *egfp* mRNA level was detected in the strain harboring pRS1-P$_{as\text{-}rnTrpL}$, while in the strain
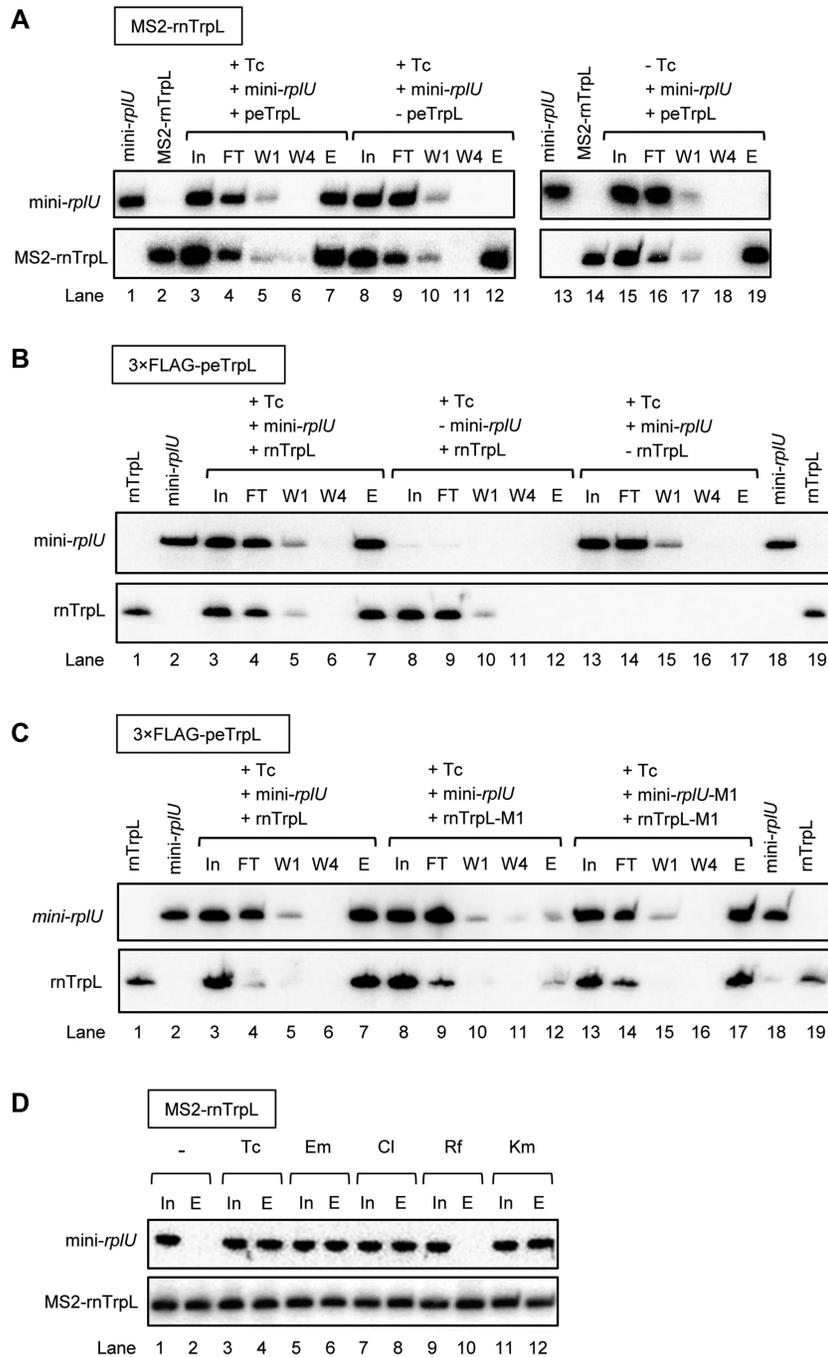
Figure 8. Reconstitution of *rplUrpmA*-ARNP. Phosphorimages showing northern blot analyses of reconstituted complexes with probes directed against rnTrpL and mini-*rplU* (indicated on the left). First the *rplU*-specific probe was used and then the membrane was rehybridized with the rnTrpL-specific probe. To detect weak signals, the blots were exposed for 40 min and some of the signals were saturated. Usage of MS2-rnTrpL or 3×FLAG-peTrpL as a bait is indicated. (**A**) Analysis of reconstituted ARNPs purified by MS2-MBP chromatography. The 50 μl reconstitution samples contained *in vitro* transcribed MS2-rnTrpL and the components indicated above the panel. After pull-down with MS2-MBP-beads, following fractions were loaded. In: input fraction (5 μl); FT: flow-through (5 μl); W1 and W4: first and last washing fractions (10 μl each); E: elution fraction (5 μl). Additionally, 10 ng of each *in vitro* transcript was loaded in the first two lanes. Copurification of MS2-rnTrpL with the mini-*rplU* transcript indicates ARNP assembly. (**B** and **C**) Analyses of reconstituted ARNPs purified by FLAG-CoIP. 1:1 (w/w) mixture of synthetic peTrpL and 3×FLAG-peTrpL, and the components indicated above the panel were used. For other descriptions see A). (**D**) Analysis of ARNPs reconstituted in the presence of the indicated antibiotics and purified by MS2-MBP chromatography. After the chromatography (the respective antibiotic was present in the washing buffer), the input and elution fractions were blotted. -: samples without antibiotic. For other descriptions see A). Two independent reconstitution experiments were performed, and the results of one of them are shown.
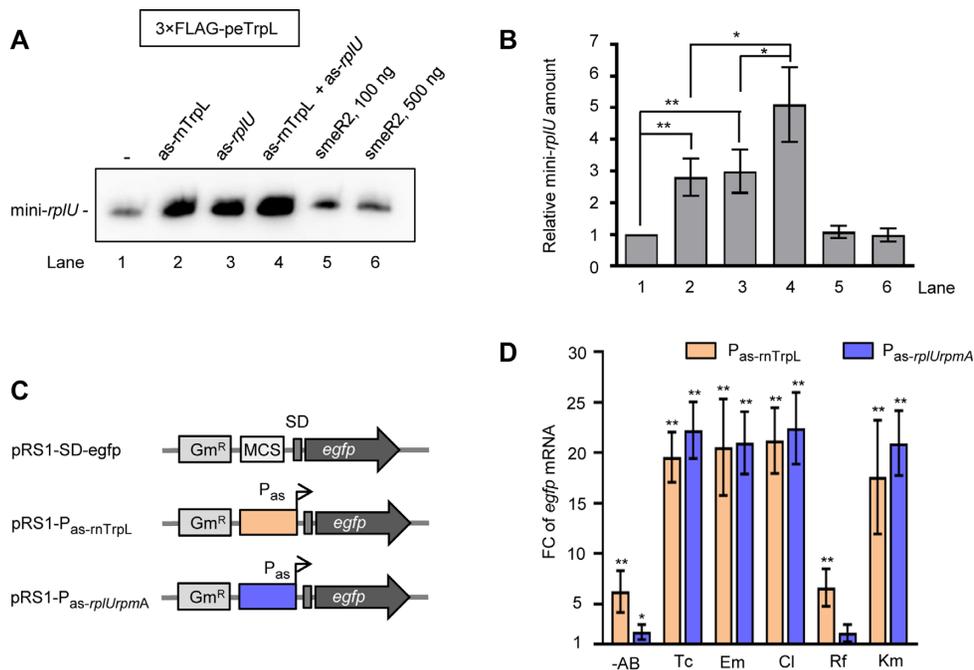
Figure 9. Antisense RNAs increase ARNP reconstitution and are induced by the inhibitors of transcription initiation. (**A**) Phosphorimage of a northern blot analysis of CoIP elution fractions after complex reconstitution. 3×FLAG-peTrpL was used as a bait (indicated). Five microliter of each fraction were loaded. Probe specific for mini-*rplU* was used for hybridization. In contrast to Figure 8, the exposure time was restricted to 15 min to enable quantitative analysis. All 50-μl reconstitution samples contained *in vitro* transcribed rnTrpL (100 ng), mini-*rplU* (100 ng), peTrpL (50 ng), 3×FLAG-peTrpL (50 ng) and 1.5 μg/ml Tc. Lane 1: elution fraction of the control sample without asRNA. To the other samples, asRNAs or a control transcript were added. Lane 2: 100 ng as-rnTrpL. Lane 3: 100 ng as-*rplU*. Lane 4: 100 ng as-rnTrpL and 100 ng as-*rplU*. Lane 5: 100 ng *smeR2* transcript (18). Lane 6: 500 ng *smeR2* transcript. (**B**) Quantitative evaluation of the phosphorimage shown in (A) and of the results from three additional, independent experiments. The bars numbering corresponds to that of the lanes in panel A). (**C**) Schemata of promoter fusion plasmids used to test for presence of antisense promoters downstream of rnTrpL and *rplUrpmA*. 300 bp-regions starting at the putative antisense TSSs (see Figure 1) were cloned upstream of the reporter *egfp*. (**D**) Antisense promoter activities induced by antibiotics in bacteria cultivated in rich TY medium. The level of the reporter *egfp* mRNA from cultures of *S. meliloti* 2011 strains containing promoter fusion constructs (see panel C) was compared to RNA from the EVC by qRT-PCR. Either no antibiotics were added (-AB), or the indicated antibiotics were added at subinhibitory concentrations and RNA was isolated 5 min thereafter. Shown are means with standard deviations from three independent experiments. According to the Student's *t*-test: *P-value ≤ 0.05; **P-value ≤ 0.01.

harboring pRS1-P$_{as-rplUrpmA}$, the *egfp* mRNA was at the detection limit (see bars labeled with'-AB' in Figure 9D). Importantly, strong induction of transcription from both cloned regions was detected 5 min after addition of Tc, Em, Cl or Km, while no induction was observed when Rf was added. This result strongly suggests the existence of antibiotic-inducible promoters of both asRNAs.

sRNA reprograming by ARNP formation

The above data collectively suggest that the rnTrpL specificity towards the *rplUrpmA* target is determined by peTrpL and a translation-inhibiting antibiotic such as Tc. To test *in vitro* whether Tc-dependent ARNP formation can redirect rnTrpL from *trpDC* to *rplUrpmA*, we decided to use mini-*trpD* and mini-*rplU in vitro* transcripts, which encompass the respective rnTrpL-binding sites (for predicted secondary structures see Supplementary Figure S7), in competition experiments.

We used native *rplUrpmA*-ARNP, which was purified from strain 2011 pRK-MS2-rnTrpL and thus harbored MS2-rnTrpL and WT peTrpL. It was present in a buffer containing 2 μg/ml Tc (High Tc conditions) and was divided in four samples (Figure 10A). The first (control) sample was diluted 5-fold maintaining the High Tc conditions,

while the second (control) sample was diluted with buffer lacking Tc to reach Low Tc conditions (0.4 μg/ml Tc), under which the ARNP is largely disassembled (see Supplementary Figure S8 showing Tc-dependent disassembly and reassembly of *rplUrpmA*-ARNP). After 10 min of incubation under High or Low Tc conditions, a pull-down experiment with MS2-MBP-beads followed by qRT-PCR analysis of *rplU* and *trpD* mRNA was conducted. As expected, *trpD* mRNA was essentially not detected, and more *rplU* mRNA was copurified with MS2-rnTrpL under High Tc conditions than under Low Tc conditions, indicating ARNP disassembly under Low Tc conditions (see 'Controls' in Figure 10A).

For the competition experiment, mini-*trpD* and mini-*rplU* transcripts were added in a ratio of 1:1 (300 ng of each transcript) to the third and fourth sample. Then, each sample was diluted to reach Low Tc conditions. After 3 min of incubation, Tc was added to one of the diluted samples to restore the High Tc conditions, while the other one was kept at Low Tc concentration. After 7 min of incubation, MS2-rnTrpL was purified together with its interaction partners from both samples, and qRT-PCR was conducted with primers detecting the mini-*trpD* and mini-*rplU* transcripts. Under low Tc conditions, mostly mini-*trpD* was co-purified (Figure 10A). In contrast, when the Tc concentration was raised, exclusively *rplU* (represented by mini-*rplU* and en-
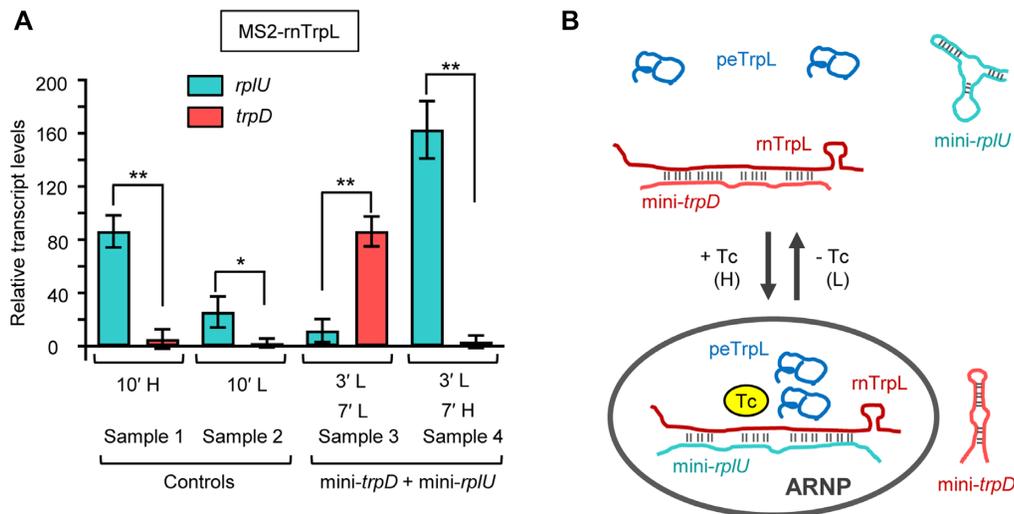
Figure 10. Tc-dependent redirection of the sRNA rnTrpL from *trpD* to *rplU*. (**A**) After purification of *rplUrpmA*-ARNP from *S. meliloti* 2011 pRK-MS2-rnTrpL grown in rich TY medium, the elution fraction was divided in four samples. They were treated differently as described in the text, and after 10 min (10′) of incubation, pull-down with MS2-MBP-beads was conducted. Copurification of the studied transcripts (indicated) with MS2-rnTrpL was analyzed by qRT-PCR. Control samples 1 and 2 were incubated under the respective conditions. To samples 3 and 4, a 1:1 mixture of mini-*trpD* and mini-*rplU in vitro* transcripts was added prior to treatment. H: High Tc conditions (2 μg/ml Tc); L: Low Tc conditions (0.4 μg/ml Tc). Shown are means and standard deviations from three independent experiments. (**B**) Schematic representation of Tc-dependent changes in the specificity of the sRNA rnTrpL as shown by complex reconstitution *in vitro*. Under Low Tc conditions, rnTrpL base pairs with *trpD*, while under High Trp conditions, the *rplU*-ARNP is formed. The stoichiometries in the complex are still unknown, but Supplementary Figure 5A and (18) suggest that peTrpL oligomerizes in the ARNP. The asRNAs were not considered in this model showing a minimal ARNP as suggested by Figure 8. According to the Student's *t*-test: *P-value $\leq$ 0.05; **P-value $\leq$ 0.01.

dogenous *rplUrpmA* that was in the ARNP) was co-purified (Figure 10A). This result provides evidence for reprogramming of the rnTrpL specificity in a Tc-dependent manner in the presence of peTrpL (Figure 10B).

Conservation of rnTrpL and peTrpL functions in other bacteria

To determine functionally important residues in peTrpL of *S. meliloti*, we performed alanine-scanning mutagenesis and tested the functionality of the mutagenized peptides in *S. meliloti* 2011. Compared to the WT peTrpL, the Ala substitution of R14 had no significant effect on the *rplUrpmA* mRNA decrease (the decrease was similar to that caused by the WT peptide; Figure 11A). This is in line with the view that the M2 mutation in rnTrpL, which leads to an R14A substitution (Figure 2A) had major impact on the sRNA-mRNA interaction because it weakens the base pairing and not because of the mutagenized peptide (Figure 5). Fig. 11A shows that the Ala substitutions of Thr4, Ser8 and Trp12, respectively, had the strongest impact. Induction of production of these mutated peptides for 10 min led to increased (rather than decreased) *rpmA* levels. The Ala substitutions of the Trp10 and Trp11 residues abolished the peTrpL effect, suggesting that all three Trp residues are important for the function of peTrpL in the *rplUrpmA*-ARNP (Figure 11A). However, EMSA of reconstituted ARNPs revealed that the labeled mini-*rplU* transcript is shifted when WT or W10A but not when W12A peptide was used (Figure 11B). Thus, at least *in vitro*, the W10A peptide supports the *rplU*-ARNP formation. The EMSA result confirmed the key role of the W12 residue in this ARNP.

Finally, we analyzed the conservation of peTrpL in the genus *Sinorhizobium* and in other Rhizobiales (Supplementary Table S4). *In silico* analysis of putative peTrpL peptides revealed several groups of conserved leader peptides that generally conform to the taxonomy (Supplementary Figure S9). However, while some of the obtained motifs are weakly similar, no features are common to all taxonomic groups, with the exception of consecutive Trp codons defining the attenuator. The consensus peTrpL sequences of the genera *Sinorhizobium, Agrobacterium* and *Bradyrhizobium* groups are shown in Figure 11C. Surprisingly, within the *Sinorhizobium* group, the functionally important residues Thr4 and Ser8 of *S. meliloti* peTrpL are less conserved than the WWWAR residues at the C-terminus of the peptide.

Despite the poor peTrpL sequence conservation, we addressed the question whether the role of rnTrpL and peTrpL in *rplUrpmA* regulation is conserved in *Agrobacterium tumefaciens* (which, together with *S. meliloti*, belongs to the *Rhizobiaceae*), and in the more distantly related *Bradyrhizobium japonicum* (a *Bradyrhizobiaceae* member). In both species, the mRNA level of *rplUrpmA* was specifically decreased when the respective peTrpL homolog Atu-peTrpL or Bja-peTrpL was overproduced from a Tc resistance-conferring plasmid (Figure 11D and Supplementary Figure S10). Thus, the function of peTrpL in the regulation of *rplUrpmA* seems to be conserved in Alphaproteobacteria.

DISCUSSION

This study shows that a small peptide and an antibiotic change the specificity of a bacterial attenuator sRNA towards ribosomal mRNA.
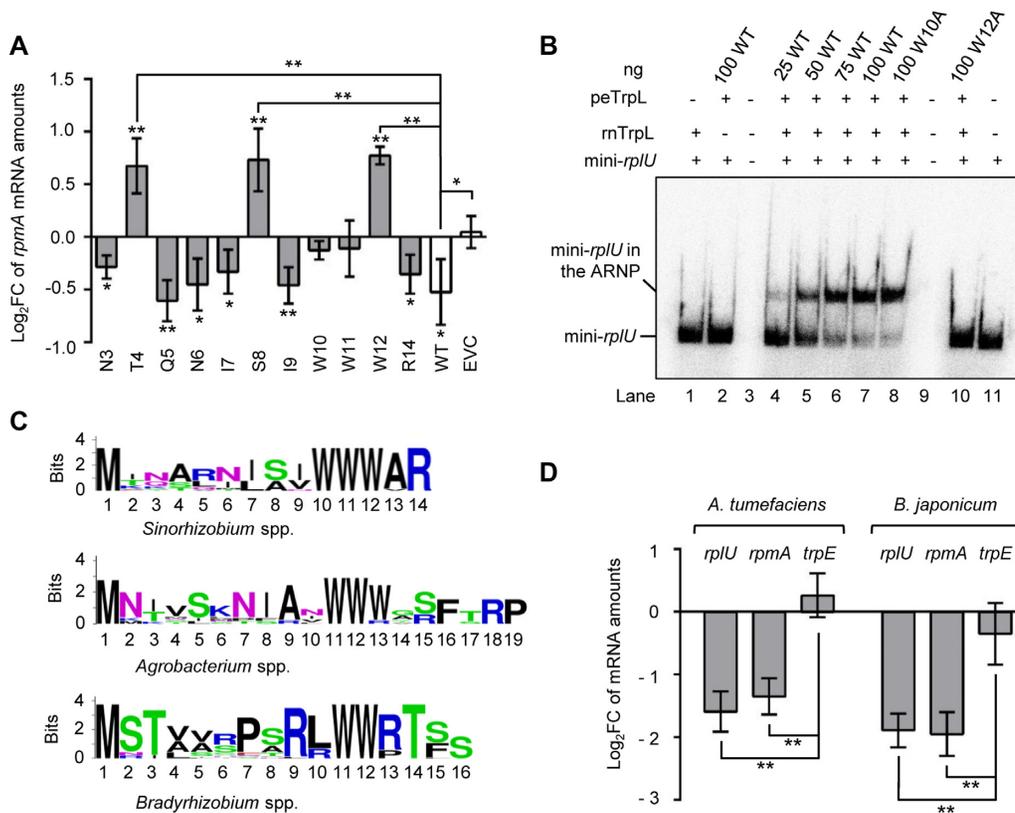
Figure 11. Conservation of peTrpL-dependent *rplUrpmA* regulation in Rhizobiales despite high divergence in peTrpL amino acid sequence. (**A**) Alanine scanning mutagenesis for analysis of functionally important residues of peTrpL in *S. meliloti* 2011. Changes in the levels of *rpmA* were determined by qRT-PCR 10 min after addition of IPTG to induce the overproduction of peTrpL variants with the indicated aa exchanges. The mRNA levels after induction were compared to those before induction. (**B**) Phosphorimage of EMSA showing the interaction between the radioactively labeled mini-*rplU* transcript with rnTrpL and peTrpL in the presence of Tc. The constituents of each reconstitution mixture containing 1.5 μg/ml Tc are indicated above the panel. WT, wild type synthetic peptide; W10A and W12A, corresponding mutated synthetic peptides. The antibiotic was also present in the native gel. Migration in the gel of labeled mini-*rplU* transcript and of this transcript in the ARNP is indicated on the left side. (**C**) Sequence logos for peTrpL of the *Sinorhizobium, Agrobacterium* and *Bradyrhizobium* groups (see Supplementary Figure S9). (**D**) qRT-PCR analysis of the indicated mRNAs in *A. tumefaciens* and *B. japonicum* shows a decrease in the *rplUrpmA* mRNA levels upon overproduction of corresponding peTrpL homologs (for overproduction of rnTrpL homologs, see Supplementary Figure S10). Plasmid pSRKTc-Atu-peTrpL was used to induce peptide production for 10 min, and mRNA levels after induction were compared to those before induction. Due to the lack of a suitable inducible system for *B. japonicum*, Bja-peTrpL was overproduced constitutively from the chromosomally integrated, Tc-resistance-conferring plasmid pRJ-Bja-rnTrpL and mRNA levels in the overproducing strain were compared to those in the EVC. The graphs show means and standard deviations from three independent experiments. According to the Student's *t*-test: *P-value ≤ 0.05; **P-value ≤ 0.01.

Peptide- and antibiotic-dependent and independent targets of rnTrpL

Most of the potential targets of the sRNA rnTrpL were predicted to interact with overlapping regions of its stem-loop 1 ([12]). Among them are *trpD* and *rplU* (Figure 2A), for which base pairing was confirmed *in vivo* (([14]) and Figure 5). However, while the interaction between *trpDC* and rnTrpL did not depend on the leader peptide peTrpL or on Tc (Figure 3B and D), both peTrpL and Tc were needed *in vivo* (Figure 3–5) and *in vitro* (Figure 8 and 10) for binding of rnTrpL to *rplUrpmA* mRNA, which resulted in mRNA destabilization (Figure 6). Our results and the previous RNA-Seq analysis of RNA that was coimmunoprecipitated with 3×FLAG-peTrpL in the presence of Tc ([18]) suggest that *rplUrpmA* mRNA is the only rnTrpL target, the binding to which depends on this antibiotic and the peptide. Surprisingly, several translation inhibitors showed similar, *trpL*-dependent effects on *rplUrpmA* mRNA (Figure 4D) and supported the

base pairing between rnTrpL and its target site in *rplU* (Figure 8D).

We were able to observe the Tc-dependent decrease in the *rplUrpmA* mRNA level in two different experimental systems: 1) in strains lacking a Tc-resistance plasmid, when Tc was added to the cultures at the subinhibitory concentration of 1.5 μg/ml (Figure 3D, Figure 4B and C), or 2) in strains harboring the Tc-resistance plasmid pRK4352 or its derivatives, which were cultured in the presence of 20 μg/ml Tc (Figure 3A–C). The Tc-resistance gene *tetA* on pRK4352 encodes an efflux pump that specifically extrudes Tc, thus lowering the cellular Tc concentration. However, the residual Tc in the cell was shown to broadly affect the transcriptome of *S. meliloti* ([18]). Our data suggest that this residual Tc concentration is sufficient to facilitate the *rplUrpmA* mRNA destabilization by peTrpL and rnTrpL (Figure 3 and 5). In fact, we discovered the principle of the here described, Tc-dependent *rplUrpmA* regulation using pRK4352-containing strains. Many experiments were

repeated with cultures of strains lacking this plasmid, to which Tc and other antibiotics were added at subinhibitory concentrations, and could confirm the results obtained in the presence of pRK4352.

Availability of peTrpL and rnTrpL upon Tc exposure

Since the rnTrpL- and peTrpL-dependent destabilization of *rplUrpmA* mRNA occurs upon exposure to subinhibitory antibiotic amounts, under such conditions the availability of both the sRNA and the peptide should be the ensured. Indeed, when 1.5 μg/ml Tc was added to *S. meliloti* cultures, rnTrpL was generated by transcription attenuation independently of the Trp availability. To demonstrate this, it was necessary to use conditions of Trp insufficiency, which we mimicked using the 2011 *ΔtrpC* mutant. How to explain the Tc-triggered transcription attenuation shown in Figure 2B and Supplementary Figure S2? In the presence of 1.5 μg/ml Tc the cells still can grow (18). Thus, under these conditions initiation of translation is not fully impaired. Instead, regular transient ribosome pausing at the *trpL* start codon in the nascent RNA is expected. Such a ribosome pausing would still allow formation of the apical stem-loop structure encompassing nucleotides 35–53 in SL1 of rnTrpL (Figure 2A). This, in turn, would allow the formation of the transcription termination structure SL3, since base-pairing between nt 46–51 and nt 88–83 in the antiterminator SL2 is needed to prevent SL3 formation (Figure 2A). This interpretation of Figure 2B is supported by the previously described superattenuation in Gammaproteobacteria, which occurs when *trpL* translation is abolished and results in the release of even more sRNA than under conditions of Trp availability (19,21–23).

Furthermore, the level of the native peTrpL was strongly increased in *S. meliloti* upon exposure to 1.5 μg/ml Tc (Figure 2C and (18)). At this subinhibitory Tc concentration *trpL* is probably still translated, although to a lesser extent. Previous results suggest that the strong increase in the peTrpL level after Tc addition is probably due to peptide stabilization in ARNP complexes (18).

In Figure 2B, the level of the Tc-induced rnTrpL (lane 4) was lower than the rnTrpL level under Trp replete conditions in minimal medium (lane 1). Despite this, rnTrpL plays a role in the response to Tc exposure in GMX minimal medium, as shown in Figure 4B and C. Also in rich TY medium relatively low rnTrpL amounts (as detected by northern blot analysis) can still influence the mRNA levels in *S. meliloti*: After 10 min induction by IPTG, in TY medium the level of the recombinant lacZ'-rnTrpL was shown to be lower than the level of native rnTrpL (14). However, such an induction was sufficient not only to downregulate *trpDC* mRNA in the absence of Tc (14), but also to decrease the level and the stability of *rplUrpmA* mRNA in the presence of Tc (Figure 3B, Figure 6A). We suggest that the low rnTrpL amounts detected in the northern blot analysis most probably reflect co-degradation of the continuously produced sRNA with its mRNA targets (42).

Implications of the *trp* attenuator response to Tc exposure

Together with (13) and (14), the data shown in Figure 2B suggest that the *S. meliloti trp* attenuator can utilize the same uORF and mutually exclusive RNA structures for two different purposes: (i) to regulate *trpE(G)* expression in response to Trp availability and (ii) to ensure rnTrpL supply for *rplUrpmA* downregulation in response to Tc exposure. This implies that the *trp* attenuator responds to (partial) inhibition of translation as an alternative signal. As explained above, this is possible because the Trp codons are located in the 3′-half of *trpL* (Figure 2A). It is known that in *E. coli*, ribosome pausing in the 5′-half of *trpL* causes transcription termination between *trpL* and *trpE*, in contrast to the ribosome pausing at the Trp codons in the 3′-half of *trpL*, which leads to formation of the antiterminator (24). Since in many attenuators of amino acid biosynthesis operons the codons relevant for antiterminator formation are located in the 3′-half of the uORF (16), such attenuators probably also respond to translation inhibiting antibiotics by sRNA release. It is conceivable that, in addition to translation inhibition, stringent response (43) could also trigger the generation of attenuator sRNAs with potential functions in *trans*. Of note, in all *Sinorhizobium* species, two asparagine and one glutamine codon(s) are located in the first half of *trpL*, which leads us to speculate that in these bacteria, the *trp* attenuator may respond to nitrogen depletion by rnTrpL liberation.

Two distinct ARNP types containing peTrpL

Despite its small size (14 aa), the peptide peTrpL has two antibiotic-related functions in *S. meliloti*: (i) the differential posttranscriptional regulation of the *smeABR* operon in response to several SmeAB-substrates (18) and (ii) the *rplUrpmA* destabilization in response to several translation inhibitors (this work). The first function is important for the bacterial multiresistance and involves *smeR*-ARNPs, which are independent of the sRNA rnTrpL. The second function relies on *rplUrpmA*-ARNPs, for which rnTrpL is indispensable.

Previously, genetic analyses, CoIP with 3×FLAG-peTrpL, pull-down with MS2-tagged RNA and *in vitro* reconstitution experiments revealed that the SmeAB-substrates Tc, Cl and Em, but not Km (which is not pumped by SmeAB), support the *smeR*-ARNP (18). Using a similar experimental strategy, in this work we have shown that the inhibitors of translation initiation Tc, Cl, Em and Km, but not Rf, which inhibits transcription initiation, support the *rplUrpmA*-ARNP (Figure 7A and 8D). This antibiotics assignment to the two ARNP types is physiologically reasonable, since in this way the SmeAB-substrates stimulate their own efflux (18), while the translation inhibitors, which can stimulate rnTrpL production, act with this sRNA to destabilize *rplUrpmA*. The discovery of two distinct ARNP types, each using several structurally different antibiotics for its assembly, was surprising and the molecular details of the ARNP structures will be studied in future.

When isolated from *S. meliloti*, both ARNP types were found to contain asRNAs. The asRNAs were first detected by RNA-Seq of RNA coimmunoprecipitated with 3×FLAG-peTrpL and were then confirmed by qRT-PCR analysis of ARNPs purified by two alternative methods, FLAG-CoIP and MS2-MBP chromatography (ref. (18), Figure 7 and Supplementary Figure S4). Additionally, in-

duction of the asRNAs upon antibiotic exposure was revealed using promoter fusion constructs (Figure 9C and D). In line with their ARNP-belonging, the asRNA complementary to *smeR* mRNA (as-*smeR* RNA) was induced by SmeAB-substrates but not by Km (18), while the as-rnTrpL and as-*rplUrpmA* RNAs were induced by the inhibitors of translation initiation but not by Rf (Figure 9D). The transcription factors responsible for the repression or induction of the particular asRNAs remain to be identified. However, induction of asRNA transcription by the same antibiotics, which support the *rplUrpmA*-ARNP formation, is in line with a function of these asRNAs in the rnTrpL- and peTrpL-dependent pathway of *rplUrpmA* regulation.

There is a major difference in the role of the asRNAs in the formation of the two ARNP types. The as-*smeR* RNA was shown to be necessary and sufficient for ARNP formation with peTrpL and Tc, suggesting that it plays a central role in *smeR* mRNA destabilization (18). In contrast, the as-rnTrpL and as-*rplUrpmA* RNAs seem to have only supportive function in the assembly of the here studied ARNP (Figure 9A and B). The central role in the *rplUrpmA*-ARNP formation was obviously occupied by the sRNA rnTrpL (Figure 8B). Indeed, complementarity between the sRNA and *rplU* was necessary for downregulation of *rplUrpmA′::egfp* expression *in vivo* (Figure 5) and for ARNP reconstitution *in vitro* (Figure 8C). However, in contrast to as-*smeR* RNA, neither rnTrpL nor the *rplU* mini-transcript could form a ternary complex with peTrpL and an antibiotic. Instead, a quaternary complex containing the sRNA, its target RNA, peTrpL and Tc was reconstituted as a minimal ARNP (Figure 8A and B).

Based on our results, we suggest that the asRNAs probably assist in unfolding of rnTrpL and of a structured *rplU* mRNA region, and that this unfolding enhances the ARNP assembly. Furthermore, we suggest that peTrpL and Tc are needed for stabilization of the sRNA-mRNA interaction in the ARNP. This suggestion is in line with the pe-TrpL dependence of the complex (Figure 8A) and with its disassembly and reassembly depending on the Tc concentration (Figure 10 and Supplementary Figure S8). Furthermore, the alanine scanning mutagenesis results (Figure 11A) suggest that in the ARNP, peTrpL adopts an alpha-helical structure, in which the surface build of the residues Tyr4, Ser8 and Trp12 is crucial for complex formation.

Despite their differences, the two ARNP types have apparent similarities: 1) involvement of peTrpL, probably as a dimer or oligomer, 2) participation of an overlapping sets of antibiotics, and 3) presence of antibiotic-inducible asRNAs. This suggests a common origin of evolution and similar molecular principles in complex formation and in destabilization of the target mRNAs. We propose the following model for adaptation to SmeAB-substrates such as Tc, Cl and Em, which are also inhibitors of translation initiation: In the presence of one of these antibiotics at a subinhibitory concentration, the rnTrpL sRNA is generated independently of the Trp availability and the peTrpL level is increased due to its involvement in two parallel, ARNP-dependent pathways: the *rplUrpmA* downregulation with the help of rnTrpL and the *smeABR* regulation leading to increased SmeAB production (Figure 12). Consequently, the SmeAB-mediated efflux causes a decrease in the intra-
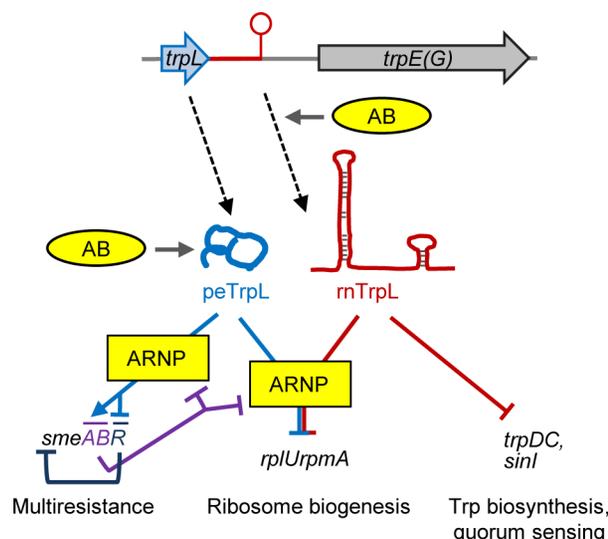
Figure 12. Model for gene regulation by the attenuator sRNA rnTrpL and the leader peptide peTrpL, the *trans*-acting products of the *trp* attenuator in *S. meliloti*. A negative effect is indicated by a color line ending with a bar and a positive effect by a color line with an arrowhead. Production of the peTrpL peptide and the rnTrpL sRNA is indicated by black, dashed arrows. Upon exposure to specific antibiotics, the amount of peTrpL and the production of rnTrpL are increased (indicated by short gray arrows labeled with AB). The rnTrpL sRNA downregulates the *trpDC* and *sinI* operons in an antibiotic- and peptide-independent manner (12,14). Upon antibiotic exposure, the peTrpL peptide differentially regulates the genes of the *smeABR* operon: While the *smeR* repressor gene is downregulated, the *smeAB* genes encoding the major MDR efflux pump are upregulated. This regulation is posttranscriptional and depends on an ARNP (antibiotic-dependent ribonucleoprotein complex) formation (18). Furthermore, upon antibiotic exposure, peTrpL and rnTrpL act together to downregulate *rplUrpmA* in an ARNP-dependent manner. The violet lines indicate that increased *smeAB* expression, which leads to antibiotic efflux, negatively influences the ARNPs, because their formation depends on the antibiotic presence in the cell.

cellular antibiotic concentration, which leads to disassembly of both ARNP types. This in turn leads to a return in *rplUrpmA* mRNA stability, higher production of the SmeR repressor and repression of *smeABR* transcription, thus accomplishing the adaptation to the antibiotic exposure.

Possible role of *rplUrpmA* destabilization upon antibiotic exposure

According to the above model, the *rplUrpmA* downregulation upon antibiotic exposure is transient and may serve to downregulate ribosome biogenesis thus saving resources for SmeAB production and antibiotic extrusion. Alternatively or in addition, it may result in ribosomes lacking the L21 and L27 proteins. The L21 proteins of *E. coli*, *Pseudomonas aeruginosa* and *S. meliloti* shows similarities between 64% and 80%; the L27 protein is more conserved, and the similarities between the L27 proteins of these species are between 80% and 85%. While the function of L21 is not clear, *E. coli* L27-deficient mutants were shown to have reduced peptidyl transferase activities (44). Interestingly, a two-fold reduction of *rplUrpmA* expression in *Pseudomonas aeruginosa* leads to an increased expression of multidrug efflux pump genes and increased resistance to aminoglycosides.

This was explained by attenuation of transcription termination, caused by pausing of L21- and L27-less ribosomes (45). Therefore, it is possible that in *S. meliloti* the *rplUrpmA* mRNA destabilization by rnTrpL and peTrpL may have similar adaptation effects mediated by specific changes in translation.

Change in target prioritization of a sRNA by small molecules

Cis-acting regulatory RNAs in mRNA leaders are known to change their structure not only in response to translation efficiency of uORFs (15) but also in response to other stimuli such as temperature (8), or due to binding to an intracellular metabolite (9) or an antibiotic (46). These and additional mechanisms can cause transcription attenuation (47), thus generating sRNAs. The regulatory potential of such sRNAs is great due to their capability to form mutually exclusive structures, but changes in the target spectrum or in prioritization of 5′-derived sRNAs were not documented yet. Interestingly, the here described change in the specificity of rnTrpL is not related to the Trp availability, which is considered the original mechanism leading to transcription termination of this sRNA. Instead, the specificity change is caused by a novel mechanism including the peTrpL peptide and specific antibiotics. This suggests that in principle, other base-pairing sRNAs could also be reprogramed by metabolites and/or (small) proteins.

Evolutionary aspects

In the evolution, sRNA reprograming was probably selected because it enlarges the target spectrum and enables the use of an sRNA that is already present in the cell for adaptation to new conditions. This would be especially useful for sRNAs such as rnTrpL, which are transcribed from housekeeping promoters. In the prototrophic strain *S. meliloti* 2011, the rnTrpL sRNA is present during growth in both rich and minimal media, because even in minimal medium, due to the *trp* genes expression, there are enough Trp-charged tRNAs to regularly cause transcription attenuation (Supplementary Figure S1). Thus, rnTrpL is well suited for reprograming in response to antibiotic stress, i.e. under conditions that *S. meliloti* regularly encounters in its soil habitat (48,49). The function of peTrpL and rnTrpL in *rplUrpmA* downregulation seems to be conserved among soil Alphaproteobacteria, such as the plant pathogen *A. tumefaciens* and the soybean symbiont *B. japonicum* (Figure 11D). The weak amino acid sequence conservation beyond the Trp residues (Figure 11C) probably reflects molecular adaptation of the peptide to the sRNA and the target mRNA in the respective host.

While peTrpL-functions were described only in *Rhizobiaceae* yet (this work and (18)), very recently it was shown that in *E. coli*, rnTrpL downregulates *dnaA* expression and thereby probably contributes to the balance between growth rate and initiation of chromosome replication (50). The here uncovered, antibiotic-related function of rnTrpL and peTrpL might be of particular importance in pathogens, because *trpL*-containing transcription attenuators are also present in pathogenic Proteobacteria of the genera *Brucella*, *Salmonella*, *Yersinia*, *Vibrio* and *Helicobacter*. Beyond

Proteobacteria, similar attenuators are found in *Corynebacterium*, *Streptomyces*, *Chlamydia* and *Deinococcus*, showing their ancient origin (17). Moreover, many bacterial species harbor several uORF-containing transcription attenuators upstream of different biosynthetic operons (16). Possible functions of the corresponding sRNAs and leader peptides still remain to be elucidated.

In summary, we show that the specificity of an attenuator sRNA is altered with the help of the leader peptide encoded by the same locus. This sRNA reprograming occurs upon antibiotic exposure. It involves the formation of an ARNP complex for downregulation of ribosomal protein genes, which probably supports bacterial adaptation. The sRNA reprograming described in this study is anticipated to inspire future investigations on alternative sRNA targets under different environmental conditions.

DATA AVAILABILITY

The MS data discussed in this publication have been deposited to the ProteomeXchange Consortium via the PRIDE partner repository (51) with the dataset identifier PXD019516.

SUPPLEMENTARY DATA

Supplementary Data are available at NAR Online.

REFERENCES

1. Cech,T.R. and Steitz,J.A. (2014) The noncoding RNA revolution-trashing old rules to forge new ones. *Cell*, **157**, 77–94.
2. Wagner,E.G.H. and Romby,P. (2015) Small RNAs in bacteria and archaea: who they are, what they do, and how they do it. *Adv. Genet.*, **90**, 133–208.

3. Durand,E., Méheust,R., Soucaze,M., Goubet,P.M., Gallina,S., Poux,C., Fobis-Loisy,I., Guillon,E., Gaude,T., Sarazin,A. *et al.* (2014) Dominance hierarchy arising from the evolution of a complex small RNA regulatory network. *Science*, **346**, 1200–1205.

4. Storz,G., Vogel,J. and Wassarman,K.M. (2011) Regulation by small RNAs in bacteria: expanding frontiers. *Mol. Cell*, **43**, 880–891.

5. Beisel,C.L., Updegrove,T.B., Janson,B.J. and Storz,G. (2012) Multiple factors dictate target selection by Hfq-binding small RNAs. *EMBO J.*, **31**, 1961–1974.

6. Witwer,K.W. and Halushka,M.K. (2016) Toward the promise of microRNAs - enhancing reproducibility and rigor in microRNA research. *RNA Biol*, **13**, 1103–1116.

7. Bobrovskyy,M., Azam,M.S., Frandsen,J.K., Zhang,J., Poddar,A., Ma,X., Henkin,T.M., Ha,T. and Vanderpool,C.K. (2019) Determinants of target prioritization and regulatory hierarchy for the bacterial small RNA SgrS. *Mol. Microbiol.*, **112**, 1199–1218.

8. Kortmann,J. and Narberhaus,F. (2012) Bacterial RNA thermometers: molecular zippers and switches. *Nat. Rev. Microbiol.*, **10**, 255–265.

9. Bédard,A.V., Hien,E.D.M. and Lafontaine,D.A. (2020) Riboswitch regulation mechanisms: RNA, metabolites and regulatory proteins. *Biochim. Biophys. Acta Gene Regul. Mech.*, **1863**, 194501.

10. Müller,P., Gimpel,M., Wildenhain,T. and Brantl,S. (2019) A new role for CsrA: promotion of complex formation between an sRNA and its mRNA target in *Bacillus subtilis*. *RNA Biol.*, **16**, 972–987.

11. Becker,A., Overlöper,A., Schlüter,J.P., Reinkensmeier,J., Robledo,M., Giegerich,R., Narberhaus,F. and Evguenieva-Hackenberg,E. (2014) Riboregulation in plant-associated α-proteobacteria. *RNA Biol.*, **11**, 550–562.

12. Baumgardt,K., Šmídová,K., Rahn,H., Lochnit,G., Robledo,M. and Evguenieva-Hackenberg,E. (2016) The stress-related, rhizobial small RNA RcsR1 destabilizes the autoinducer synthase encoding mRNA *sinI* in *Sinorhizobium meliloti*. *RNA Biol*, **13**, 486–499.

13. Bae,Y.M. and Crawford,I.P. (1990) The *Rhizobium meliloti trpE(G)* gene is regulated by attenuation, and its product, anthranilate synthase, is regulated by feedback inhibition. *J. Bacteriol.*, **172**, 3318–3327.

14. Melior,H., Li,S., Madhugiri,R., Stötzel,M., Azarderakhsh,S., Barth-Weber,S., Baumgardt,K., Ziebuhr,J. and Evguenieva-Hackenberg,E. (2019) Transcription attenuation-derived small RNA rnTrpL regulates tryptophan biosynthesis gene expression in *trans*. *Nucleic Acids Res.*, **47**, 6396–6410.

15. Yanofsky,C. (1981) Attenuation in the control of expression of bacterial operons. *Nature*, **289**, 751–758.

16. Vitreschak,A.G., Lyubetskaya,E.V., Shirshin,M.A., Gelfand,M.S. and Lyubetsky,V.A. (2004) Attenuation regulation of amino acid biosynthetic operons in proteobacteria: comparative genomics analysis. *FEMS Microbiol. Lett.*, **234**, 357–370.

17. Merino,E., Jensen,R.A. and Yanofsky,C. (2008) Evolution of bacterial *trp* operons and their regulation. *Curr. Opin. Microbiol.*, **11**, 78–86.

18. Melior,H., Maaß,S., Li,S., Förstner,K.U., Azarderakhsh,S., Varadarajan,A.R., Stötzel,M., Elhossary,M., Barth-Weber,S., Ahrens,C.H. *et al.* (2020) The leader peptide peTrpL forms antibiotic-containing ribonucleoprotein complexes for posttranscriptional regulation of multiresistance genes. *mBio*, **11**, e01027-20.

19. Lee,F. and Yanofsky,C. (1977) Transcription termination at the *trp* operon attenuators of *Escherichia coli* and *Salmonella typhimurium*: RNA secondary structure and regulation of termination. *Proc. Natl. Acad. Sci. U.S.A.*, **74**, 4365–4369.

20. Bae,Y.M. and Stauffer,G.V. (1991) Genetic analysis of the attenuator of the *Rhizobium meliloti trpE(G)* gene. *J. Bacteriol.*, **173**, 3382–3388.

21. Yanofsky,C. and Horn,V. (1994) Role of regulatory features of the trp operon of *Escherichia coli* in mediating a response to a nutritional shift. *J. Bacteriol.*, **176**, 6245–6254.

22. Roesser,J.R., Nakamura,Y. and Yanofsky,C. (1989) Regulation of basal level expression of the tryptophan operon of Escherichia coli. *J. Biol. Chem.*, **264**, 12284–12288.

23. Stroynowski,I., van Cleemput,M. and Yanofsky,C. (1982) Superattenuation in the tryptophan operon of *Serratia marcescens*. *Nature*, **298**, 38–41.

24. Zurawski,G., Elseviers,D., Stauffer,G.V. and Yanofsky,C. (1978) Translational control of transcription termination at the attenuator of the *Escherichia coli* tryptophan operon. *Proc. Natl. Acad. Sci. U.S.A.*, **75**, 5988–5992.

25. Beringer,J.E. (1974) R factor transfer in *Rhizobium leguminosarum*. *J. Gen. Microbiol.*, **84**, 188–198.

26. Schlüter,J.P., Reinkensmeier,J., Daschkey,S., Evguenieva-Hackenberg,E., Janssen,S., Jänicke,S., Becker,J.D., Giegerich,R. and Becker,A. (2010) A genome-wide survey of sRNAs in the symbiotic nitrogen-fixing alpha-proteobacterium *Sinorhizobium meliloti*. *BMC Genomics*, **11**, 245.

27. Mesa,S., Hauser,F., Friberg,M., Malaguti,E., Fischer,H.M. and Hennecke,H. (2008) Comprehensive assessment of the regulons controlled by the FixLJ-FixK$_2$-FixK$_1$ cascade in *Bradyrhizobium japonicum*. *J. Bacteriol.*, **190**, 6568–6579.

28. Sambrook,J., Fritsch,E.F. and Maniatis,T. (1989) In: *Molecular Cloning: A Laboratory Manual. 2*. Cold Spring Harbor Laboratory Press, NY.

29. Mank,N.N., Berghoff,B.A., Hermanns,Y.N. and Klug,G. (2012) Regulation of bacterial photosynthesis genes by the small noncoding RNA PcrZ. *Proc. Natl. Acad. Sci. U.S.A.*, **109**, 16306–11631.

30. Khan,S.R., Gaines,J., Roop,R.M. 2nd and Farrand,S.K. (2008) Broad-host-range expression vectors with tightly regulated promoters and their use to examine the influence of TraR and TraM expression on Ti plasmid quorum sensing. *Appl. Environ. Microbiol.*, **74**, 5053–5062.

31. Pfaffl,M.W. (2001) A new mathematical model for relative quantification in real-time RT-PCR. *Nucleic Acids Res.*, **29**, e45.

32. Said,N., Rieder,R., Hurwitz,R., Deckert,J., Urlaub,H. and Vogel,J. (2009) In vivo expression and purification of aptamer-tagged small RNA regulators. *Nucleic Acids Res.*, **37**, e133.

33. Schägger,H. (2006) Tricine-SDS-PAGE. *Nat. Protoc.*, **1**, 16–22.

34. Rossmann,F.M., Rick,T., Mrusek,D., Sprankel,L., Dörrich,A.K., Leonhard,T., Bubendorfer,S., Kaever,V., Bange,G. and Thormann,K.M. (2019) The GGDEF domain of the phosphodiesterase PdeB in *Shewanella putrefaciens* mediates recruitment to the polar landmark protein HubP. *J. Bacteriol.*, **201**, e00534-18.

35. Bonn,F., Bartel,J., Büttner,K., Hecker,M., Otto,A. and Becher,D. (2014) Picking vanished proteins from the void: how to collect and ship/share extremely dilute proteins in a reproducible and highly efficient manner. *Anal. Chem.*, **86**, 7421–7427.

36. MacLean,B., Tomazela,D.M., Shulman,N., Chambers,M., Finney,G.L., Frewen,B., Kern,R., Tabb,D.L., Liebler,D.C. and MacCoss,M.J. (2010) Skyline: an open source document editor for creating and analyzing targeted proteomics experiments. *Bioinformatics*, **26**, 966–968.

37. Benson,D.A., Cavanaugh,M., Clark,K., Karsch-Mizrachi,I., Lipman,D.J., Ostell,J. and Sayers,E.W. (2013) GenBank. *Nucleic Acids Res*, **41**, D36–D42.

38. Crooks,G.E., Hon,G., Chandonia,J.M. and Brenner,S.E. (2004) WebLogo: a sequence logo generator. *Genome Res.*, **14**, 1188–1190.

39. Mann,M., Wright,P.R. and Backofen,R. (2017) IntaRNA 2.0: enhanced and customizable prediction of RNA-RNA interactions. *Nucleic Acids Res.*, **45**, W435–W439.

40. Zuker,M. (2003) Mfold web server for nucleic acid folding and hybridization prediction. *Nucleic Acids Res.*, **31**, 3406–3415.

41. Schlüter,J.P., Reinkensmeier,J., Barnett,M.J., Lang,C., Krol,E., Giegerich,R., Long,S.R. and Becker,A. (2013) Global mapping of transcription start sites and promoter motifs in the symbiotic α-proteobacterium *Sinorhizobium meliloti* 1021. *BMC Genomics*, **14**, 156.

42. Massé,E., Escorcia,F.E. and Gottesman,S. (2003) Coupled degradation of a small regulatory RNA and its mRNA targets in *Escherichia coli*. *Genes Dev.*, **17**, 2374–2383.

43. Goldman,E. and Jakubowski,H. (1990) Uncharged tRNA, protein synthesis, and the bacterial stringent response. *Mol. Microbiol.*, **4**, 2035–2040.

44. Maguire,B.A., Beniaminov,A.D., Ramu,H., Mankin,A.S. and Zimmermann,R.A. (2005) A protein component at the heart of an RNA machine: the importance of protein L27 for the function of the bacterial ribosome. *Mol. Cell*, **20**, 427–435.

45. Lau,C.H., Fraud,S., Jones,M., Peterson,S.N. and Poole,K. (2012) Reduced expression of the *rplU-rpmA* ribosomal protein operon in *mexXY*-expressing pan-aminoglycoside-resistant mutants of

Pseudomonas aeruginosa. Antimicrob. Agents Chemother., **56**, 5171–5179.

46. Jia,X., Zhang,J., Sun,W., He,W., Jiang,H., Chen,D. and Murchie,A.I. (2013) Riboswitch control of aminoglycoside antibiotic resistance. *Cell*, **152**, 68–81.

47. Turnbough,C.L. Jr (2019) Regulation of bacterial gene expression by transcription attenuation. *Microbiol. Mol. Biol. Rev.*, **83**, e00019-19.

48. Eda,S., Mitsui,H. and Minamisawa,K. (2011) Involvement of the SmeAB multidrug efflux pump in resistance to plant antimicrobials and contribution to nodulation competitiveness in *Sinorhizobium meliloti. Appl. Environ. Microbiol.*, **77**, 2855–2862.

49. Walsh,F. and Duffy,B. (2013) The culturable soil antibiotic resistome: a community of multi-drug resistant bacteria. *PLoS One*, **8**, e65567.

50. Li,S., Edelmann,D., Berghoff,B.A., Georg,J. and Evguenieva-Hackenberg,E. (2020) Bioinformatic prediction reveals posttranscriptional regulation of the chromosomal replication initiator gene *dnaA* by the attenuator sRNA rnTrpL in *Escherichia coli. RNA Biol*, **19**, 1–15.

51. Vizcaíno,J.A., Csordas,A., del-Toro,N., Dianes,J.A., Griss,J., Lavidas,I., Mayer,G., Perez-Riverol,Y., Reisinger,F., Ternent,T. *et al.* (2016) 2016 update of the PRIDE database and its related tools. *Nucleic Acids Res.*, **44**, D447–D456.